

A modulator of the low-voltage activated T-type calcium channel that reverses HIV glycoprotein 120-, paclitaxel-, and spinal nerve ligation-induced peripheral neuropathies

Song Cai^{‡,¶}, Peter Tuohy^{†,¶}, Chunlong Ma[†], Naoya Kitamura[†], Kimberly Gomez[‡], Yuan Zhou[‡], Dongzhi Ran[‡], Shreya Sai Bellampalli^{‡,a}, Jie Yu[‡], Shizhen Luo[‡], Angie Dorame[‡], Nancy Yen Ngan Pham[‡], Gabriella Molnar[‡], John M. Streicher[‡], Marcel Patek[‡], Samantha Perez-Miller[‡], Aubin Moutal[‡], Jun Wang^{†,*}, and Rajesh Khanna^{‡,#,¥,Δ,*}

[†]Department of Pharmacology and Toxicology, College of Pharmacy, The University of Arizona, Tucson, Arizona 85721, United States

[‡]Department of Pharmacology, College of Medicine, The University of Arizona, Tucson, Arizona, 85721, United States

[‡]Bright Rock Path Consulting LLC, Tucson, AZ

[#]BIO5 Institute, 1657 East Helen Street, P.O. Box 210240, Tucson, AZ 85721, United States

[¥]The Center for Innovation in Brain Sciences, The University of Arizona Health Sciences, Tucson, Arizona, United States

^ΔRegulonix LLC, Tucson, Arizona, United States

[¶]These authors contributed equally

Expanded Materials and Methods

Animals.

Pathogen-free adult male and female Sprague-Dawley rats (225-250g; Envigo, Indianapolis, IN) were housed in temperature-controlled (23±3 °C) and light-controlled (12-h light/12-h dark cycle; lights on 07:00-19:00) rooms with standard rodent chow and water available ad libitum. The Institutional Animal Care and Use Committee of the College of Medicine at the University of Arizona approved all experiments. All procedures were conducted in accordance with the Guide for Care and Use of Laboratory Animals published by the National Institutes of Health and the ethical guidelines of the International Association for the Study of Pain. Animals were randomly assigned to treatment or control groups for the behavioral experiments. Animals were initially housed 3 per cage but individually housed after the intrathecal cannulation. All behavioral

experiments were performed by experimenters who were blinded to the experimental groups and treatments.

Preparation of acutely dissociated dorsal root ganglion neurons

Dorsal root ganglia from all levels were acutely dissociated using methods as described previously [6]. Rat DRG neurons were isolated from 100g female Sprague-Dawley rats using previously developed procedures [13]. In brief, removing dorsal skin and muscle and cutting the vertebral bone processes parallel to the dissection stage exposed the DRGs. DRGs were then collected, trimmed at their roots, and enzymatically digested in 3 mL bicarbonate-free, serum-free, sterile DMEM (Cat# 11965, Thermo Fisher Scientific, Waltham, MA) solution containing neutral protease (3.125 mg.ml⁻¹, Cat#LS02104; Worthington, Lakewood, NJ) and collagenase type I (5 mg/mL, Cat# LS004194, Worthington, Lakewood, NJ) and incubated for 60 minutes at 37°C under gentle agitation. Dissociated DRG neurons (~1.5 x 10⁶) were then gently centrifuged to collect cells and washed with DRG media DMEM containing 1% penicillin/streptomycin sulfate from 10,000 µg/mL stock, 30 ng/mL nerve growth factor, and 10% fetal bovine serum before plating onto poly-D-lysine- and laminin-coated glass 12- or 15-mm coverslips.

Calcium imaging in acutely dissociated dorsal root ganglion neurons

Dorsal root ganglion neurons were loaded for 30 minutes at 37°C with 3 µM Fura-2AM (Cat# F1221, Thermo Fisher, stock solution prepared at 1mM in DMSO, 0.02% pluronic acid, (Cat#P-3000MP, Thermo Fisher) to follow changes in intracellular calcium([Ca²⁺]_i) in a standard bath solution containing 139 mM NaCl, 3 mM KCl, 0.8 mM MgCl₂, 1.8 mM CaCl₂, 10 mM Na HEPES, pH 7.4, 5 mM glucose exactly as previously described [1]. Fluorescence imaging was performed with an inverted microscope, NikonEclipseTi-U (Nikon Instruments Inc., Melville, NY), using objective Nikon Fluor 4X and a Photometrics cooled CCD camera CoolSNAPES² (Roper Scientific, Tucson, AZ) controlled by NIS Elements software (version 4.20, Nikon Instruments). The excitation light was delivered by a Lambda-LS system (Sutter Instruments, Novato, CA). The excitation filters (340 ± 5 and 380 ± 7) were controlled by a Lambda 10 to 2 optical filter change (Sutter Instruments). Fluorescence was recorded through a 505-nm dichroic mirror at 535 ± 25 nm.

To minimize photobleaching and phototoxicity, the images were taken every ~10 seconds during the time-course of the experiment using the minimal exposure time that provided acceptable image quality. The changes in $[Ca^{2+}]_c$ were monitored by following a ratio of F_{340}/F_{380} , calculated after subtracting the background from both channels.

Dorsal root ganglia neuron transfection.

Collected cells were re-suspended in Nucleofector transfection reagent containing siRNA at 500 nM and 2 μ g of the provided GFP plasmid as detailed previously [4]. Cells were then subjected to electroporation protocol O-003 in an Amaxa Biosystem (Lonza, Basel, Switzerland) and plated onto poly-D-lysine - and laminin-coated glass 12-mm coverslips. Transfection efficiencies were routinely between 20% and 30% with ~10% cell death. Small diameter neurons were selected to target A δ - and c- fiber nociceptive neurons. For rat DRG culture small cells were considered to be $\sim < 30 \mu$ m as determined by an eyepiece micrometer within the objective lens. Successfully transfected cells were identified by GFP fluorescence. The siRNA sequences used were: UAGAUAGCAAUACUUUGGCCGGGG (for *Cacna1g*/CaV3.1; (Cat# RSS355855, Thermofisher)); CAGCCAUCUUCGUGGUGGAGAUGAU (for *Cacna1h*/CaV3.2; (Cat# RSS350286, Thermofisher)); CAGCAUCCUUGGGAUGCAUAUCUUU (for *Cacna1i*/CaV3.3; Cat# RSS367566); and siRNA Negative Control, Med GC was used as a scrambled siRNA control (Cat# 12935300). Cells were used 48 hrs after transfection.

Constellation Pharmacology.

These experiments were performed as described previously [13; 19], but with the following modifications. Dorsal root ganglia neurons were loaded at 37°C with 3 μ M Fura-2AM for 30 minutes in Tyrode solution (at ~310 mOsm) containing 119 mM NaCl, 2.5 mM KCl, 2 mM MgCl₂, 2 mM CaCl₂, 25 mM HEPES, pH 7.4, and 30 mM glucose. After a 1-minute baseline measurement, Ca²⁺ influx was stimulated by the addition of the following receptor agonists: 400 nM menthol, 50 μ M histamine, 10 μ M adenosine triphosphate (ATP), 200 μ M allyl isothiocyanate (AITC), 1 mM acetylcholine (Ach), and 100 nM capsaicin diluted in Tyrode solution. At the end of the constellation pharmacology protocol, cell viability was assessed by depolarization-induced Ca²⁺

influx using and an excitatory KCl solution comprising 32 mM NaCl, 90 mM KCl, 2 mM MgCl₂, 2 mM CaCl₂, 25 mM HEPES, pH 7.4, and 30 mM glucose. After the 1-minute baseline measurement, each trigger was applied for 15 seconds in the order indicated above in 6-minute intervals. After each trigger, bath solution was continuously perfused over the cells to wash off excess of the trigger. This process was automated using the ValveBank II perfusion system that controlled the perfusion of the standard bath solution and triggers (Automate Scientific, San Diego, CA). Except for the time course experiments, **5bk** was incubated overnight onto DRGs. In all cases, **5bk** was *also* added to the Tyrode solution during the loading with Fura-2AM. Fluorescence imaging was performed under the same conditions noted above for calcium imaging. A cell was defined as a “responder” if its fluorescence ratio of 340 nm/380 nm was greater than 10% of the baseline value calculated using the average fluorescence in the 30 seconds preceding application of the trigger.

Whole-cell patch recordings of Ca²⁺ and Na⁺ currents in acutely dissociated DRG neurons.

Recordings were obtained from acutely dissociated DRG neurons as described previously [9; 14]. To isolate calcium currents, Na⁺ and K⁺ currents were blocked with 500 nM tetrodotoxin (TTX; Alomone Laboratories) and 30 mM tetraethylammonium chloride (TEA-Cl; Sigma). Extracellular recording solution (at ~310 mOsm) consisted of the following (in mM): 110 *N*-methyl-D-glucamine (NMDG), 10 BaCl₂, 30 TEA-Cl, 10 HEPES, 10 glucose, pH at 7.4, 0.001 TTX, 0.01 nifedipine. The intracellular recording solution (at ~310 mOsm) consisted of the following (in mM): 150 CsCl₂, 10 HEPES, 5 Mg-ATP, 5 BAPTA, pH at 7.4. The protocol for isolating T-type calcium currents was previously described by Choe et al.[3] The extracellular recording solution used to isolate T currents consisted of the following (in millimolar): 2 CaCl₂, 152 TEA-Cl, 10 HEPES, pH adjusted to 7.4 with TEA-OH. The intracellular recording solution consisted of (in millimolar): 135 tetramethylammonium hydroxide, 10 EGTA, 40 HEPES, and 2 MgCl₂, pH adjusted to 7.2 with hydrofluoric acid. Activation of I_{Ca-T} was measured by using a holding voltage of -90 mV with voltage steps 200 ms in duration applied at 500-ms intervals in 10 mV increments from -70 to +60 mV. Inactivation of I_{Ca-T} was determined by applying a 1500-ms conditioning prepulse (-110 to +20 mV in 10 mV increments) after which the voltage was stepped to -30 mV for 20 ms; a 40-ms interval with a holding voltage of -90 mV separated each acquisition. In the

deactivation tau protocol, the neuron was first held at -110 mV, then the voltage jumped to -30 mV for 10 ms followed by a 50-ms conditioning prepulse (-160 to -40 mV in 10 mV increments). A 2-second interval with a holding voltage of -90 mV separated each acquisition. I_{Ca-T} recovery from inactivation were obtained by using our standard double-pulse protocol with variable interpulse duration at -90 mV after a 500-ms-long inactivating pulse ($V_h = -90$ mV; $V_t = -30$ mV).

To isolate the contributions of the HVA calcium channel subtypes, we applied all but one of the following subunit-selective blockers (all purchased from Alomone Labs, Jerusalem): Nifedipine (10 μ M, L-type); ω -agatoxin GIVA (200 nM, P/Q-type) [12]; SNX-482 (200 nM, R-type) [16]; ω -conotoxin GVIA (500 nM, N-type) [7] or TTA-P2 (1 μ M, T-type) [3] to individually isolate the subtypes.

For recording sodium currents the internal solution consisted of (in mM): 140 CsF, 10 NaCl, 1.1 Cs-EGTA, and 15 HEPES (pH 7.3, mOsm/L = 290-310) and external solution contained (in mM): 140 NaCl, 30 tetraethylammonium chloride, 10 D-glucose, 3 KCl, 1 CaCl₂, 0.5 CdCl₂, 1 MgCl₂, and 10 HEPES (pH 7.3, mOsm/L = 310-315). DRG neurons were interrogated with current-voltage (I-V) and activation/inactivation voltage protocols as previously described [4; 6]. The voltage protocols were as follows: (a) I-V protocol: from a -60 mV holding potential, cells were depolarized in 150-millisecond voltage steps from -70 to $+60$ mV (5-mV increments) which permitted acquisition of current density values such that we could analyze activation of sodium channels as a function of current vs voltage and infer peak current density (normalized to cell capacitance (in picofarads, pF)), which occurred between ~ 0 to 10 mV; (b) inactivation protocol: from a -60 mV holding potential, cells were subjected to hyperpolarizing/repolarizing pulses for 1 second between -120 to 0 mV ($+10$ mV steps). This increment conditioned various proportions of channels into a state of fast-inactivation – in this case 0-mV test pulse for 200 milliseconds was able to reveal fast inactivation when normalized to maximum sodium current. Because of the differential inactivation kinetics of TTX-resistant and TTX-sensitive channels, the fast inactivation protocol allowed subtraction of electrically isolated TTX-R (current available after -40 mV prepulse) from total current (current available after -120 mV prepulse), as previously described [4]. Pipettes with 1 to 3 M Ω resistance were used for all recordings.

The Boltzmann relation was used to determine the voltage dependence for activation of I_{Ca} and I_{Na} wherein the conductance–voltage curve was fit by the equation $G/G_{max} = 1/[1 + \exp(V_{0.5} -$

$V_m/k]$, where G is the conductance $G=I/(V_m-E_{Ca}$ or $E_{Na})$, G_{max} is the maximal conductance obtained from the Boltzmann fit under control conditions, $V_{0.5}$ is the voltage for half-maximal activation, V_m is the membrane potential, and k is a slope factor. E_{Ca} is the reversal potential for I_{Ca} ; E_{Na} is the reversal potential for I_{Na} and was determined for each individual neuron. The values of I_{Ca} and I_{Na} around the reversal potential were fit with a linear regression line to establish the voltage at which the current was zero. The Boltzmann parameters were determined for each individual neuron and then used to calculate the mean \pm SEM.

Whole-cell recordings were obtained with a HEKA EPC-10 USB (HEKA Instruments Inc.); data were acquired with a Patchmaster (HEKA) and analyzed with a Fitmaster (HEKA). Capacitive artifacts were fully compensated, and series resistance was compensated by $\sim 70\%$. Recordings made from cells with greater than a 5-mV shift in series resistance compensation error were excluded from analysis. All experiments were performed at room temperature ($\sim 23^\circ\text{C}$). Pipettes with 1-3M Ω resistance were used for all recordings.

Calcitonin gene-related peptide release from lumbar slices.

Rats were deeply anesthetized with 5% isoflurane and then decapitated. Two vertebral incisions (cervical and lumbar) were made in order to expose the spinal cord. Pressure was applied to a saline-filled syringe inserted into the lumbar vertebral foramen, and the spinal cord was extracted. Only the lumbar region of the spinal cord was used for the CGRP release assay. Baseline treatments (#1 and #2) involved bathing the spinal cord in Tyrode's solution. The excitatory solution consisting of 90 mM KCl was paired with the treatment for fraction #4. These fractions (10 minutes, 400 μL each) were collected for measurement of CGRP release. Samples were immediately flash frozen and stored in a -20°C freezer. **5bk** (20 μM) or vehicle (0.9% saline) was added to the pretreatment and co-treatment fractions (#3 and 4). The concentration of CGRP released into the buffer was measured by enzyme-linked immunosorbant assay (Cat# 589001, Cayman Chemical, Ann Arbor, MI).

Preparation of spinal cord slices.

As described previously [22], young rats (postnatal 10-14 days) were deeply anesthetized with diethyl ether. For spinal nerve blocking, 0.3 mL of 2% lidocaine was injected to both sides of L4 to 5 lumbar vertebrae. Laminectomy was performed from mid-thoracic to low lumbar levels, and the spinal cord was quickly removed to cold modified artificial cerebrospinal fluid (aCSF) oxygenated with 95% O₂ and 5% CO₂. The aCSF contained (in millimolar): 80 NaCl, 2.5 KCl, 1.25 NaH₂PO₄, 0.5 CaCl₂, 3.5 MgCl₂, 25 NaHCO₃, 75 sucrose, 1.3 ascorbate, 3.0 sodium pyruvate, with pH at 7.4 and osmolarity at 310 mOsm. Transverse 350- μ m thick slices were obtained by a vibratome (VT1200S; Leica, Nussloch, Germany). Slices were then incubated for at least 1 hour at RT in an oxygenated recording solution containing (in millimolar): 125 NaCl, 2.5 KCl, 2 CaCl₂, 1 MgCl₂, 1.25 NaH₂PO₄, 26 NaHCO₃, 25 D-glucose, 1.3 ascorbate, 3.0 sodium pyruvate, with pH at 7.4 and osmolarity at 320 mOsm. The slices were then positioned in a recording chamber and continuously perfused with oxygenated recording solution at a rate of 3 to 4 mL/min before electrophysiological recordings at RT.

Electrophysiological recording in spinal cord slices by whole-cell patch clamp.

Substantia gelatinosa neurons were visualized and identified in the slices by means of infrared differential interference contrast video microscopy on an upright microscope (FN1; Nikon, Tokyo, Japan) equipped with a 340/0.80 water-immersion objective and a charge-coupled device camera. Patch pipettes with resistance at 6 to 10 M Ω were made from borosilicate glass (Sutter Instruments, Novato, CA) on a 4-steps micropipette puller (P-90; Sutter Instruments, Novato, CA). The pipette solution contained the following (in millimolar): 120 potassium gluconate, 20 KCl, 2 MgCl₂, 2 Na₂-ATP, 0.5 Na-GTP, 20 HEPES, 0.5 EGTA, with pH at 7.28 and osmolarity at 310 mOsm. The membrane potential was held at -60 mV using PATCHMASTER software in combination with a patch clamp amplifier (EPC10; HEKA Elektronik, Lambrecht, Germany).

The whole-cell configuration was obtained in voltage-clamp mode. To record spontaneous excitatory postsynaptic currents (sEPSCs), bicuculline methiodide (10 μ M) and strychnine (1 μ M) were added to the recording solution to block γ -aminobutyric acid-activated and glycine-activated currents. **5bk** was applied for 2-3 hours prior to the recordings. Hyperpolarizing step pulses (5 mV in intensity, 50 milliseconds in duration) were periodically delivered to monitor the access

resistance (15-25 M Ω), and recordings were discontinued if the access resistance changed by more than 20%. For each neuron, sEPSCs were recorded for a total duration of 2 minutes. Currents were filtered at 3 kHz and digitized at 5 kHz. Data were further analyzed by the Mini-Analysis (Synatosoft Inc, NJ) and Clampfit 10.7 Program. The amplitude and frequency of sEPSCs were compared between neurons from animals in control and **5bk** groups.

Implantation of intrathecal catheter.

For intrathecal (i.t.) drug administration, rats were chronically implanted with catheters as described by Yaksh and Rudy [21]. Rats were anesthetized with ketamine/xylazine and placed in a stereotactic head holder. The occipital muscles were separated from their occipital insertion and retracted caudally to expose the cisternal membrane at the base of the skull. Polyethylene tubing was passed caudally from the cisterna magna to the level of the lumbar enlargement. Animals were allowed to recover and were examined for evidence of neurologic injury. Animals with evidence of neuromuscular deficits were excluded.

Testing of allodynia.

The assessment of tactile allodynia (i.e., a decreased threshold to paw withdrawal after probing with normally innocuous mechanical stimuli) consisted of testing the withdrawal threshold of the paw in response to probing with a series of calibrated fine (von Frey) filaments. Each filament was applied perpendicularly to the plantar surface of the paw of rats held in suspended wire mesh cages. Withdrawal threshold was determined by sequentially increasing and decreasing the stimulus strength (the “up and down” method), and data were analyzed with the nonparametric method of Dixon, as described by Chaplan et al [2] and expressed as the mean withdrawal threshold.

HIV sensory neuropathy (HIV SN).

Mechanical allodynia was produced by intrathecal administration of the human immunodeficiency virus-1 (HIV-1) envelope glycoprotein, GP120 [11]. Seven days after implantation of an intrathecal catheter, baseline behavioral measurements were obtained and then rats were randomly

assigned to two groups. On days 10, 12 and 14, rats were injected i.t. with 300 ng of GP120 (Cat#4961, HIV-1 BaL gp120 recombinant protein, NIH-AIDS Reagent program) in a final volume of 20 μ l in 0.9% saline and 0.1% BSA. Rats were tested on day 35 (i.e., 21 days after the last i.t. injection of GP120).

Paclitaxel-induced neuropathy model.

Rats were given paclitaxel (Cat# P-925-1, Goldbio, Olivette, MO) based on the protocol described by Polomano et al. [18]. In brief, pharmaceutical-grade paclitaxel (Taxol) was resuspended at a concentration of 2 mg/ml in 30% 1:1 Cremophor EL: ethanol, 70% Saline and given to the rats at 2 mg/kg intraperitoneally (i.p.) every other day for a total of 4 injections (days 0, 2, 4, and 6), resulting in a final cumulative dose of 8 mg/kg. No abnormal spontaneous behavioral changes in the rats were noted during or after the treatment. Animals developed mechanical hyperalgesia within 10 days after the first paclitaxel injection.

Elevated Plus Maze (EPM).

The EPM consists of four elevated (50cm) arms (50cm long and 10cm wide) with two opposing arms containing 30cm high opaque walls. EPM testing occurred in a quiet testing room with ambient lighting at ~500 lux. On day of testing, rats were allowed to acclimate to the testing room for 20 minutes. Each rat was placed in a closed arm, facing the enter platform and cage mates started in the same closed arm. Each rat was allowed 5 minutes to explore the EPM and then returned to its home cage. Between animals the EPM was cleaned thoroughly with Versa-Clean (Fisher Scientific). EPM performance was recorded using an overhead video camera (MHD Sport 2.0 WiFi Action Camera, Walmart.com) for later quantification. Open and closed arm entries were defined as the front two paws entering the arm, and open arm time began the moment the front paws entered the open arm and ended upon exit. An anxiety index was also calculated; the index combines EPM parameters into one unified ratio with values ranging from 0 to 1, with a higher value indicating increased anxiety [8]. The following equation was used for calculation of the anxiety index:

Anxiety Index = $1 - (\text{open arm time}/5 \text{ min}) + (\text{open arm entry}/\text{total entry})$

Spinal nerve ligation (SNL).

Nerve ligation, performed as described earlier [10; 13], produces signs of neuropathic dysesthesias, including tactile allodynia and thermal hypersensitivity. All nerve operations occurred 5 days after intrathecal catheter implantation. Rats were anesthetized with 2% isoflurane in O₂ anesthesia delivered at 2 L/min. The skin over the caudal lumbar region was incised and the muscles retracted. The L₅ and L₆ spinal nerves were exposed, carefully isolated, and tightly ligated with 4-0 silk distal to the dorsal root ganglion without limiting the use of the left hind paw of the animal. All animals were allowed 7 days to recover before any behavioral testing. Any animals exhibiting signs of motor deficiency were euthanized.

Rotarod.

Rats were trained to walk on a rotating rod (10 rev/min; Rotamex 4/8 device) with a maximal cutoff time of 180 seconds. Training was initiated by placing the rats on a rotating rod and allowing them to walk until either falling off, or maximal cutoff time was reached. This process was repeated 6 times and the rats were allowed to recover for 24 hours before intrathecal compound administration. Prior to treatment, the rats were run once on a moving rod in order to establish a baseline value. Assessment consisted of placing the rats on the moving rod and timing until either they fell off or reached a maximum of 180 seconds.

Competition Radioligand Binding

Details on our cell lines, culture methods, and binding methods have been reported previously [17]. All cells were Chinese Hamster Ovary (CHO-K1) cells overexpressing human opioid receptor (μ [MOR], δ [DOR], or κ [KOR]). Cell pellets for binding were prepared by growing cells to confluency in 15 cm dishes, 3 per pellet. The cells were collected using 5 mM EDTA in dPBS (no trypsin) and stored at -80°C until the assay was performed. The assay was performed by incubating 18.5-25 μ g of membrane protein with 0.97-4.76 nM of ³H-diprenorphine (PerkinElmer)

and concentration curves of **5bk** or positive control (naloxone for MOR and DOR, U50,488 for KOR) in a 200 μ L volume for 1 hour at room temperature. Reactions were harvested using a 96 well format Brandel Cell Harvester, and data acquired using a PerkinElmer MicroBeta2 6-detector 96-well format scintillation counter. The data was normalized to binding in the presence of Vehicle (100%; 0.1% DMSO and 0.1% BSA) and non-specific binding (0%; 10 μ M naloxone) and reported as the mean \pm SEM. Curves were fit using a 1-site binding 3-variable nonlinear regression model with GraphPad Prism 8.3, using the previously-measured K_D values of ^3H -diprenorphine in these cells [17]. The data output was reported as the mean $K_i \pm$ SEM of $N=3$ independent experiments.

Statistical Analysis.

All data was first tested for a Gaussian distribution using a D'Agostino-Pearson test (Prism 8 Software, Graphpad, San Diego, CA). SNI- (day 15 post-surgery), GP120- (day 15 post last injection) and paclitaxel- (day 15 post-injection) induced allodynia was quantified as percentage of maximum possible allodynia using the formula: percentage allodynia = [(baseline threshold – post-injury threshold)/baseline threshold] \times 100. Reversal of allodynia by drugs (that is, anti-allodynia) was quantified with respect to the area under the threshold-time curve (using the trapezoidal method) over the post-injection testing period. Data are reported as percentage of the maximum possible anti-allodynia, calculated for each rat as a ratio of its actual anti-allodynia compared to a hypothetical situation in which the drug brought withdrawal thresholds to their original baseline at all post-injection time points. The statistical significance of differences between means was determined by a parametric ANOVA followed by Tukey's post hoc or a non-parametric Kruskal Wallis test followed by Dunn's post-hoc test depending on if datasets achieved normality. Behavioral data with a time course were analyzed by Two-way ANOVA with Sidak's post hoc test. Differences were considered significant if $p \leq 0.05$. Error bars in the graphs represent mean \pm SEM. See statistical analysis described in Table 1. All data were plotted in Prism 8. No outlier data were removed.

Chemistry. Chemicals were ordered from commercial sources and were used without further purification. Synthesis procedures for reactions described in Scheme 1 were shown below. All

final compounds were purified by flash column chromatography. ^1H and ^{13}C NMR spectra were recorded on a Bruker-400 NMR spectrometer. Chemical shifts are reported in parts per million referenced with respect to residual solvent (CD_3OD) 3.31 ppm, ($\text{DMSO}-d_6$) 2.50 ppm, and (CDCl_3) 7.24 ppm or from internal standard tetramethylsilane (TMS) 0.00 ppm. The following abbreviations were used in reporting spectra: s, singlet; d, doublet; t, triplet; q, quartet; m, multiplet; dd, doublet of doublets; ddd, doublet of doublet of doublets. All reactions were carried out under N_2 atmosphere unless otherwise stated. HPLC-grade solvents were used for all reactions. Flash column chromatography was performed using silica gel (230–400 mesh, Merck). Low-resolution mass spectra were obtained using an ESI technique on a 3200 Q Trap LC/MS/MS system (Applied Biosystems). The purity was assessed by using a Shimadzu LC-MS with a Waters XTerra MS C-18 column (part no. 186000538), 50 mm \times 2.1 mm, at a flow rate of 0.3 mL/min; $\lambda = 250$ and 220 nm; mobile phase A, 0.1% formic acid in H_2O , and mobile phase B', 0.1% formic in 60% 2-propanol, 30% CH_3CN , and 9.9% H_2O . All compounds submitted for mechanistic studies were confirmed to be >95.0% purity by LC-MS traces.

Synthesis procedures.

General procedure for the synthesis of tetrazole. Aldehyde (1 mmol) and amine (1 mmol) were added to methanol (5ml). The solution was stirred at room temperature for 10 mins. Then TMS- N_3 (1 mmol) and isocyanide (1 mmol) were added sequentially. The mixture was stirred at room temperature overnight. Solvent was removed by rotatory evaporation and the crude product was purified by flash column chromatography (20-100% ethyl acetate/hexane) to give the final product.

1- $\{1-(2,6\text{-dimethylphenyl})\text{-}1\text{H}\text{-}1,2,3,4\text{-tetrazol}\text{-}5\text{-yl}\}(5\text{-methylthiophen}\text{-}2\text{-yl})\text{methyl}\}\text{-}4\text{-}(\text{furan}\text{-}2\text{-carbonyl})\text{piperazine}$. (**5aa**). Yield: 90.6%. ^1H NMR (400 MHz, CDCl_3) δ 7.51 – 7.33 (m, 2H), 7.29 – 7.20 (m, 1H), 7.20 – 7.09 (m, 1H), 6.94 (dd, $J = 3.4, 0.9$ Hz, 1H), 6.66 (d, $J = 3.5$ Hz, 1H), 6.56 (dt, $J = 3.6, 1.2$ Hz, 1H), 6.44 (dd, $J = 3.4, 1.8$ Hz, 1H), 4.70 (s, 1H), 3.88 – 3.60 (m, 4H), 2.85 – 2.62 (m, 2H), 2.58 – 2.45 (m, 2H), 2.43 (s, 3H), 2.05 (s, 3H), 1.53 (s, 3H). ^{13}C NMR (101 MHz, CDCl_3) δ 158.92, 154.74, 147.71, 143.72, 142.24, 136.41, 135.63, 132.82, 131.48, 131.18, 129.07, 128.96, 128.92, 124.78, 116.54, 111.29, 58.95, 50.27, 17.70, 16.95, 15.36. $\text{C}_{24}\text{H}_{26}\text{N}_6\text{O}_2\text{S}$, EI-MS: m/z ($\text{M}+\text{H}^+$): 463.6 (calculated), 463.6 (found).

1-(furan-2-carbonyl)-4-[(5-methylthiophen-2-yl)($\{1-[(1\text{S})\text{-}1\text{-phenylethyl}]\text{-}1\text{H}\text{-}1,2,3,4\text{-tetrazol}\text{-}5\text{-yl}\}$)methyl]piperazine. (**5ab**). Yield: 71.9%. ^1H NMR (400 MHz, CDCl_3) δ 7.46 – 7.38 (m, 1H), 7.38 – 7.27 (m, 3H), 7.24 – 7.12 (m, 2H), 6.92 (dd, $J = 3.5, 0.8$ Hz, 0.5H), 6.88 (dd, $J = 3.5, 0.9$ Hz, 0.5H), 6.64 (d, $J = 3.5$ Hz, 0.5H), 6.60 (dd, $J = 3.2, 0.8$ Hz, 1H), 6.54 – 6.49 (m, 0.5H), 6.45 – 6.36 (m, 1H), 6.08 (q, $J = 7.1$ Hz, 0.5H), 5.54 (q, $J = 7.0$ Hz, 0.5H), 5.11 (s, 0.5H), 5.06 (s,

0.5H), 3.77 – 3.44 (m, 4H), 2.67 – 2.53 (m, 1H), 2.53 – 2.40 (m, 4H), 2.40 – 2.23 (m, 2H), 2.02 – 1.89 (m, 3H). ¹³C NMR (101 MHz, CDCl₃) δ 158.94, 158.88, 153.52, 153.32, 147.80, 147.77, 143.76, 143.67, 142.05, 141.78, 139.73, 139.23, 132.92, 132.90, 129.26, 129.16, 129.04, 128.77, 128.67, 128.61, 126.33, 126.10, 124.90, 124.79, 116.64, 116.43, 111.35, 111.27, 60.35, 59.35, 59.11, 58.84, 50.53, 49.66, 22.79, 15.42, 15.37. C₂₄H₂₆N₆O₂S, EI-MS: m/z (M+H⁺): 463.6 (calculated), 463.6 (found).

1-[(1-benzyl-1H-1,2,3,4-tetrazol-5-yl)(5-methylthiophen-2-yl)methyl]-4-(furan-2-carbonyl)piperazine. (**5ac**). Yield: 74.9%. ¹H NMR (400 MHz, CDCl₃) δ 7.42 (dd, *J* = 1.8, 0.9 Hz, 1H), 7.39 – 7.28 (m, 3H), 7.20 – 7.09 (m, 2H), 6.93 (dd, *J* = 3.5, 0.8 Hz, 1H), 6.64 (d, *J* = 3.5 Hz, 1H), 6.58 (dt, *J* = 3.5, 1.1 Hz, 1H), 6.43 (dd, *J* = 3.5, 1.7 Hz, 1H), 5.74 (d, *J* = 15.4 Hz, 1H), 5.48 (d, *J* = 15.4 Hz, 1H), 5.07 (s, 1H), 3.76 – 3.58 (m, 4H), 2.67 – 2.51 (m, 2H), 2.43 (s, 3H), 2.44 – 2.32 (m, 2H). ¹³C NMR (101 MHz, CDCl₃) δ 158.97, 153.78, 147.82, 143.77, 142.04, 133.42, 132.58, 129.30, 129.07, 128.91, 127.52, 124.93, 116.66, 111.38, 59.72, 51.55, 50.09, 15.43. C₂₃H₂₄N₆O₂S, EI-MS: m/z (M+H⁺): 449.5 (calculated), 449.5 (found).

1-[(1-cyclohexyl-1H-1,2,3,4-tetrazol-5-yl)(5-methylthiophen-2-yl)methyl]-4-(furan-2-carbonyl)piperazine. (**5ad**). Yield: 85.1%. ¹H NMR (400 MHz, CDCl₃) δ 7.43 (dd, *J* = 1.8, 0.9 Hz, 1H), 6.96 (dd, *J* = 3.5, 0.9 Hz, 1H), 6.77 (d, *J* = 3.5 Hz, 1H), 6.60 (dq, *J* = 3.4, 1.1 Hz, 1H), 6.44 (dd, *J* = 3.5, 1.8 Hz, 1H), 5.26 (s, 1H), 4.57 – 4.39 (m, 1H), 3.96 – 3.59 (m, 4H), 2.78 – 2.66 (m, 2H), 2.62 – 2.47 (m, 2H), 2.45 (s, 3H), 2.13 – 1.85 (m, 6H), 1.85 – 1.64 (m, 2H), 1.48 – 1.30 (m, 2H). ¹³C NMR (101 MHz, CDCl₃) δ 159.08, 152.64, 147.84, 143.80, 141.89, 133.91, 128.65, 124.97, 116.75, 111.41, 60.23, 58.55, 50.63, 33.15, 33.10, 25.56, 25.50, 24.91, 15.46. C₂₂H₂₈N₆O₂S, EI-MS: m/z (M+H⁺): 441.6 (calculated), 441.6 (found).

1-(furan-2-carbonyl)-4-({1-[(4-methylbenzenesulfonyl)methyl]-1H-1,2,3,4-tetrazol-5-yl}(5-methylthiophen-2-yl)methyl)piperazine. (**5ae**). Yield: 80.9%. ¹H NMR (400 MHz, CDCl₃) δ 7.58 – 7.46 (m, 2H), 7.43 (dd, *J* = 1.8, 0.9 Hz, 1H), 7.36 – 7.28 (m, 2H), 6.95 (dd, *J* = 3.5, 0.9 Hz, 1H), 6.84 (d, *J* = 3.5 Hz, 1H), 6.72 – 6.60 (m, 1H), 6.43 (dd, *J* = 3.5, 1.8 Hz, 1H), 6.15 (d, *J* = 14.4 Hz, 1H), 5.73 (s, 1H), 5.55 (d, *J* = 14.4 Hz, 1H), 4.00 – 3.66 (m, 4H), 2.75 – 2.55 (m, 4H), 2.47 (s, 3H), 2.44 (s, 3H). ¹³C NMR (101 MHz, CDCl₃) δ 158.95, 154.97, 147.74, 147.05, 143.80, 142.27, 132.28, 130.56, 130.20, 129.81, 128.95, 124.99, 116.73, 111.37, 65.89, 59.41, 49.56, 21.90, 15.40. C₂₄H₂₆N₆O₄S₂, EI-MS: m/z (M+H⁺): 527.6 (calculated), 527.4 (found).

1-(furan-2-carbonyl)-4-[(5-methylthiophen-2-yl)(1-pentyl-1H-1,2,3,4-tetrazol-5-yl)methyl]piperazine. (**5af**). Yield: 62.3%. ¹H NMR (400 MHz, CDCl₃) δ 7.43 (dd, *J* = 1.8, 0.9 Hz, 1H), 6.96 (dd, *J* = 3.5, 0.9 Hz, 1H), 6.78 (d, *J* = 3.5 Hz, 1H), 6.61 (dq, *J* = 3.4, 1.1 Hz, 1H), 6.44 (dd, *J* = 3.5, 1.8 Hz, 1H), 5.28 (s, 1H), 4.44 – 4.26 (m, 2H), 3.95 – 3.68 (m, 4H), 2.88 – 2.72 (m, 2H), 2.65 – 2.49 (m, 2H), 2.44 (s, 3H), 1.93 – 1.76 (m, 2H), 1.40 – 1.22 (m, 4H), 0.87 (t, *J* = 6.9 Hz, 3H). ¹³C NMR (101 MHz, CDCl₃) δ 159.00, 153.19, 147.76, 143.83, 142.19, 128.97, 125.04, 116.79, 111.42, 59.74, 50.36, 48.01, 29.32, 28.67, 22.18, 15.44, 13.90. C₂₁H₂₈N₆O₂S, EI-MS: m/z (M+H⁺): 429.6 (calculated), 429.5 (found).

1-(furan-2-carbonyl)-4-[(5-methylthiophen-2-yl)[1-(naphthalen-2-yl)-1H-1,2,3,4-tetrazol-5-yl]methyl]piperazine. (**5ag**). Yield: 74.5%. ¹H NMR (400 MHz, CDCl₃) δ 8.03 (dt, *J* = 8.6, 0.7 Hz, 1H), 8.01 – 7.91 (m, 2H), 7.91 – 7.82 (m, 1H), 7.71 – 7.59 (m, 2H), 7.50 (dd, *J* = 8.7, 2.2 Hz,

1H), 7.43 (dd, $J = 1.8, 0.9$ Hz, 1H), 6.95 (dd, $J = 3.4, 0.9$ Hz, 1H), 6.79 (d, $J = 3.5$ Hz, 1H), 6.63 (dq, $J = 3.3, 1.0$ Hz, 1H), 6.44 (dd, $J = 3.5, 1.8$ Hz, 1H), 5.26 (s, 1H), 3.92 – 3.64 (m, 4H), 2.94 – 2.69 (m, 2H), 2.65 – 2.50 (m, 2H), 2.47 (s, 3H). ^{13}C NMR (101 MHz, CDCl_3) δ 159.01, 147.77, 143.79, 133.74, 132.86, 130.82, 130.37, 128.50, 128.33, 128.18, 128.02, 125.02, 124.68, 122.37, 116.69, 111.38, 58.67, 49.67, 15.48. $\text{C}_{26}\text{H}_{24}\text{N}_6\text{O}_2\text{S}$, EI-MS: m/z ($\text{M}+\text{H}^+$): 485.6 (calculated), 485.6 (found).

1-[(1-tert-butyl-1H-1,2,3,4-tetrazol-5-yl)(5-methylthiophen-2-yl)methyl]-4-(furan-2-carbonyl)piperazine. (**5ah**). Yield: 79.3%. ^1H NMR (400 MHz, CDCl_3) δ 7.42 (dd, $J = 1.8, 0.9$ Hz, 1H), 6.94 (dd, $J = 3.4, 0.9$ Hz, 1H), 6.65 (d, $J = 3.5$ Hz, 1H), 6.57 (dq, $J = 3.4, 1.1$ Hz, 1H), 6.43 (dd, $J = 3.5, 1.8$ Hz, 1H), 5.57 (s, 1H), 3.91 – 3.63 (m, 4H), 3.01 – 2.81 (m, 2H), 2.66 – 2.52 (m, 2H), 2.44 (s, 3H), 1.73 (s, 9H). ^{13}C NMR (101 MHz, CDCl_3) δ 159.02, 153.29, 147.85, 143.74, 142.21, 129.12, 124.75, 116.57, 111.34, 61.78, 60.10, 49.89, 30.26, 15.44. $\text{C}_{20}\text{H}_{26}\text{N}_6\text{O}_2\text{S}$, EI-MS: m/z ($\text{M}+\text{H}^+$): 415.5 (calculated), 415.3 (found).

1-(furan-2-carbonyl)-4-[[1-(4-methoxyphenyl)-1H-1,2,3,4-tetrazol-5-yl](5-methylthiophen-2-yl)methyl]piperazine. (**5ai**). Yield: 79.5%. ^1H NMR (400 MHz, CDCl_3) δ 7.42 (dd, $J = 1.8, 0.9$ Hz, 1H), 7.34 – 7.27 (m, 2H), 7.08 – 6.99 (m, 2H), 6.94 (dd, $J = 3.5, 0.9$ Hz, 1H), 6.76 – 6.68 (m, 1H), 6.63 – 6.55 (m, 1H), 6.43 (dd, $J = 3.5, 1.8$ Hz, 1H), 5.14 (s, 1H), 3.88 (s, 3H), 3.84 – 3.66 (m, 4H), 2.92 – 2.71 (m, 2H), 2.56 – 2.47 (m, 2H), 2.45 (s, 3H). ^{13}C NMR (101 MHz, CDCl_3) δ 161.36, 159.01, 153.45, 147.81, 143.78, 128.94, 126.95, 126.07, 124.96, 116.64, 115.10, 111.37, 58.60, 55.84, 49.73, 15.46. $\text{C}_{23}\text{H}_{24}\text{N}_6\text{O}_3\text{S}$, EI-MS: m/z ($\text{M}+\text{H}^+$): 465.5 (calculated), 465.4 (found).

1-[[1-(2,6-dimethylphenyl)-1H-1,2,3,4-tetrazol-5-yl](5-methylfuran-2-yl)methyl]-4-(furan-2-carbonyl)piperazine. (**5aj**). Yield: 85.3%. ^1H NMR (400 MHz, CDCl_3) δ 7.43 (dd, $J = 1.8, 0.9$ Hz, 1H), 7.37 (t, $J = 7.6$ Hz, 1H), 7.25 – 7.21 (m, 1H), 7.18 – 7.13 (m, 1H), 6.93 (dd, $J = 3.5, 0.9$ Hz, 1H), 6.43 (dd, $J = 3.5, 1.8$ Hz, 1H), 6.33 (dt, $J = 3.2, 0.5$ Hz, 1H), 5.92 – 5.87 (m, 1H), 3.81 – 3.67 (m, 4H), 2.90 – 2.77 (m, 2H), 2.52 – 2.38 (m, 2H), 2.22 (s, 3H), 2.04 (s, 3H), 1.64 (s, 3H). ^{13}C NMR (101 MHz, CDCl_3) δ 159.02, 153.55, 153.32, 147.80, 145.02, 143.79, 136.13, 136.00, 131.69, 131.17, 128.96, 116.63, 112.98, 111.36, 106.74, 56.79, 50.28, 17.77, 17.10, 13.74. $\text{C}_{24}\text{H}_{26}\text{N}_6\text{O}_3$, EI-MS: m/z ($\text{M}+\text{H}^+$): 447.5 (calculated), 447.5 (found).

1-(furan-2-carbonyl)-4-[[5-(methylsulfanyl)thiophen-2-yl]({1-[(1S)-1-phenylethyl]-1H-1,2,3,4-tetrazol-5-yl})methyl]piperazine. (**5ak**). Yield: 79.6%. ^1H NMR (400 MHz, CDCl_3) δ 7.47 – 7.40 (m, 1H), 7.40 – 7.25 (m, 3H), 7.25 – 7.11 (m, 2H), 6.95 (dd, $J = 3.5, 0.8$ Hz, 0.5H), 6.93 – 6.84 (m, 1H), 6.80 (d, $J = 3.7$ Hz, 0.5H), 6.73 (d, $J = 3.6$ Hz, 0.5H), 6.62 (d, $J = 3.7$ Hz, 0.5H), 6.49 – 6.36 (m, 1H), 6.04 (q, $J = 7.0$ Hz, 0.5H), 5.64 (q, $J = 7.0$ Hz, 0.5H), 5.15 (s, 0.5H), 5.13 (s, 0.5H), 3.85 – 3.65 (m, 2H), 3.65 – 3.42 (m, 2H), 2.68 – 2.56 (m, 1H), 2.49 (s, 1.5H), 2.47 (s, 1.5H), 2.53 – 2.32 (m, 3H), 2.12 – 1.95 (m, 3H). ^{13}C NMR (101 MHz, CDCl_3) δ 158.93, 158.85, 152.98, 152.81, 147.69, 147.67, 143.80, 143.71, 139.94, 139.64, 139.60, 139.08, 137.03, 137.01, 129.69, 129.46, 129.26, 129.23, 129.22, 128.91, 128.78, 126.22, 126.07, 116.73, 116.53, 111.37, 111.29, 60.08, 59.28, 59.18, 58.94, 50.34, 49.56, 22.84, 22.69, 21.65, 21.50. $\text{C}_{24}\text{H}_{26}\text{N}_6\text{O}_2\text{S}_2$, EI-MS: m/z ($\text{M}+\text{H}^+$): 495.6 (calculated), 495.8 (found).

1-(furan-2-carbonyl)-4-({1-[(1S)-1-phenylethyl]-1H-1,2,3,4-tetrazol-5-yl})(thiophen-2-yl)methyl)piperazine. (**5al**). Yield: 78.4%. ¹H NMR (400 MHz, CDCl₃) δ 7.48 – 7.39 (m, 1H), 7.39 – 7.24 (m, 4H), 7.24 – 7.12 (m, 2H), 7.02 – 6.90 (m, 1.5H), 6.90 – 6.84 (m, 1H), 6.84 – 6.77 (m, 0.5H), 6.49 – 6.35 (m, 1H), 6.10 (q, *J* = 7.0 Hz, 0.5H), 5.68 (q, *J* = 7.0 Hz, 0.5H), 5.28 (s, 1H), 3.82 – 3.63 (m, 2H), 3.63 – 3.35 (m, 2H), 2.71 – 2.52 (m, 1H), 2.52 – 2.29 (m, 3H), 2.01 – 1.89 (m, 3H). ¹³C NMR (101 MHz, CDCl₃) δ 158.75, 158.66, 153.25, 153.04, 147.51, 147.50, 143.66, 143.57, 139.63, 138.94, 135.32, 135.16, 129.04, 128.99, 128.77, 128.59, 128.53, 127.02, 126.79, 126.61, 126.54, 126.14, 125.96, 116.40, 116.21, 111.18, 111.10, 59.56, 58.89, 58.69, 58.66, 50.19, 49.33, 22.67, 22.50. C₂₃H₂₄N₆O₂S, EI-MS: *m/z* (M+H⁺): 449.5 (calculated), 449.6 (found).

1-{{1-(2,6-dimethylphenyl)-1H-1,2,3,4-tetrazol-5-yl}(thiophen-2-yl)methyl}-4-(furan-2-carbonyl)piperazine. (**5am**). Yield: 86.4%. ¹H NMR (400 MHz, CDCl₃) δ 7.42 (dd, *J* = 1.8, 0.9 Hz, 1H), 7.39 (t, *J* = 7.6 Hz, 1H), 7.34 – 7.28 (m, 1H), 7.28 – 7.21 (m, 1H), 7.17 – 7.09 (m, 1H), 6.98 – 6.88 (m, 3H), 6.43 (dd, *J* = 3.5, 1.8 Hz, 1H), 4.81 (s, 1H), 3.94 – 3.64 (m, 4H), 2.90 – 2.66 (m, 2H), 2.57 – 2.42 (m, 2H), 2.05 (s, 3H), 1.48 (s, 3H). ¹³C NMR (101 MHz, CDCl₃) δ 158.98, 154.69, 147.82, 143.80, 136.48, 135.75, 135.37, 131.50, 131.32, 129.28, 129.08, 129.06, 127.59, 126.93, 116.70, 111.40, 58.74, 50.38, 17.83, 16.96. C₂₃H₂₄N₆O₂S, EI-MS: *m/z* (M+H⁺): 449.5 (calculated), 449.5 (found).

1-{{1-(2,6-dimethylphenyl)-1H-1,2,3,4-tetrazol-5-yl}(thiophen-3-yl)methyl}-4-(furan-2-carbonyl)piperazine. (**5an**). Yield: 81.6%. ¹H NMR (400 MHz, CDCl₃) δ 7.42 (dd, *J* = 1.8, 0.9 Hz, 1H), 7.38 (t, *J* = 7.6 Hz, 1H), 7.30 – 7.20 (m, 2H), 7.15 – 7.02 (m, 3H), 6.95 (dd, *J* = 3.5, 0.9 Hz, 1H), 6.44 (dd, *J* = 3.5, 1.8 Hz, 1H), 4.59 (s, 1H), 3.91 – 3.66 (m, 4H), 2.81 – 2.56 (m, 2H), 2.56 – 2.36 (m, 2H), 2.03 (s, 3H), 1.36 (s, 3H). ¹³C NMR (101 MHz, CDCl₃) δ 158.97, 147.84, 143.80, 136.62, 135.53, 131.55, 131.25, 129.06, 129.00, 128.13, 126.89, 116.71, 111.41, 59.43, 50.84, 17.80, 16.75. C₂₃H₂₄N₆O₂S, EI-MS: *m/z* (M+H⁺): 449.5 (calculated), 449.5 (found).

1-(furan-2-carbonyl)-4-[phenyl({1-[(1S)-1-phenylethyl]-1H-1,2,3,4-tetrazol-5-yl})methyl]piperazine. (**5ao**). Yield: 68.9%. ¹H NMR (400 MHz, CDCl₃) δ 7.47 – 7.38 (m, 1H), 7.38 – 7.27 (m, 6H), 7.27 – 7.18 (m, 2H), 7.17 – 7.05 (m, 2H), 6.96 – 6.84 (m, 1H), 6.47 – 6.35 (m, 1H), 5.93 (q, *J* = 7.0 Hz, 0.5H), 5.47 (q, *J* = 7.1 Hz, 0.5H), 4.92 (s, 0.5H), 4.79 (s, 0.5H), 3.82 – 3.50 (m, 4H), 2.69 – 2.55 (m, 0.5H), 2.49 – 2.26 (m, 3.5H), 1.96 – 1.81 (m, 3H). ¹³C NMR (101 MHz, CDCl₃) δ 158.82, 158.74, 154.00, 153.62, 147.64, 143.67, 143.59, 139.47, 138.82, 133.71, 133.60, 129.16, 128.97, 128.92, 128.87, 128.66, 128.62, 128.60, 128.50, 126.30, 125.95, 116.43, 116.27, 111.22, 111.16, 64.55, 64.44, 58.59, 58.52, 53.49, 50.87, 50.37, 22.45, 22.43. C₂₅H₂₆N₆O₂, EI-MS: *m/z* (M+H⁺): 443.5 (calculated), 443.6 (found).

1-{{1-(2,6-dimethylphenyl)-1H-1,2,3,4-tetrazol-5-yl}(2-methylphenyl)methyl}-4-(furan-2-carbonyl)piperazine. (**5ap**). Yield: 76.3%. ¹H NMR (400 MHz, CDCl₃) δ 7.42 (dd, *J* = 1.8, 0.9 Hz, 1H), 7.40 – 7.29 (m, 2H), 7.26 – 7.19 (m, 1H), 7.17 – 7.04 (m, 2H), 7.04 – 6.98 (m, 2H), 6.96 (dd, *J* = 3.4, 0.9 Hz, 1H), 6.44 (dd, *J* = 3.5, 1.8 Hz, 1H), 4.64 (s, 1H), 3.86 (s, 4H), 2.77 – 2.64 (m, 2H), 2.62 – 2.50 (m, 2H), 2.00 (s, 3H), 1.68 (s, 3H), 0.97 (s, 3H). ¹³C NMR (101 MHz, CDCl₃) δ 158.96, 156.13, 147.86, 143.78, 137.37, 137.32, 134.93, 131.48, 131.26, 130.76, 130.14, 129.11, 128.83, 126.86, 116.65, 111.38, 60.73, 51.29, 18.72, 17.69, 16.19. C₂₆H₂₈N₆O₂, EI-MS: *m/z* (M+H⁺): 457.6 (calculated), 457.6 (found).

1-(furan-2-carbonyl)-4-({1-[(1S)-1-phenylethyl]-1H-1,2,3,4-tetrazol-5-yl})(thian-4-yl)methyl)piperazine. (**5aq**). Yield: 62.8%. ¹H NMR (400 MHz, CDCl₃) δ 7.48 – 7.24 (m, 5H), 7.23 – 7.12 (m, 1H), 6.95 (dd, *J* = 3.5, 0.9 Hz, 0.5H), 6.86 (dd, *J* = 3.4, 0.9 Hz, 0.5H), 6.50 – 6.35 (m, 1H), 5.63 – 5.45 (m, 1H), 4.00 – 3.35 (m, 5H), 2.76 – 2.33 (m, 7H), 2.33 – 1.98 (m, 6H), 1.50 – 1.22 (m, 2H), 0.90 – 0.76 (m, 0.5H), 0.40 – 0.17 (m, 0.5H). ¹³C NMR (101 MHz, CDCl₃) δ 159.01, 158.94, 152.38, 151.30, 147.70, 143.81, 143.67, 139.65, 139.61, 129.39, 129.36, 129.09, 128.99, 126.37, 126.18, 116.79, 116.40, 111.41, 111.27, 63.43, 63.06, 59.03, 58.75, 38.85, 37.99, 31.90, 31.41, 31.07, 28.48, 28.34, 28.27, 28.06, 23.68, 22.95. C₂₄H₃₀N₆O₂S, EI-MS: *m/z* (M+H⁺): 467.6 (calculated), 467.6 (found).

1-{{1-(2,6-dimethylphenyl)-1H-1,2,3,4-tetrazol-5-yl}(phenyl)methyl}-4-(furan-2-carbonyl)piperazine. (**5ar**). Yield: 90.3%. ¹H NMR (400 MHz, CDCl₃) δ 7.42 (dd, *J* = 1.8, 0.9 Hz, 1H), 7.37 (t, *J* = 7.6 Hz, 1H), 7.31 – 7.18 (m, 4H), 7.17 – 7.10 (m, 2H), 7.09 – 7.02 (m, 1H), 6.95 (dd, *J* = 3.5, 0.9 Hz, 1H), 6.43 (dd, *J* = 3.5, 1.8 Hz, 1H), 4.38 – 4.24 (m, 1H), 4.01 – 3.67 (m, 4H), 2.70 – 2.45 (m, 4H), 2.02 (s, 3H), 1.09 (s, 3H). ¹³C NMR (101 MHz, CDCl₃) δ 158.95, 147.87, 143.78, 136.94, 135.03, 131.48, 131.25, 129.54, 129.24, 129.07, 128.94, 128.90, 116.68, 111.40, 65.35, 51.52, 17.76, 16.60. C₂₅H₂₆N₆O₂, EI-MS: *m/z* (M+H⁺): 443.5 (calculated), 443.6 (found).

1-{{1-[1-(2,6-dimethylphenyl)-1H-1,2,3,4-tetrazol-5-yl]-2-phenylethyl}-4-(furan-2-carbonyl)piperazine. (**5as**). Yield: 83.9%. ¹H NMR (400 MHz, CDCl₃) δ 7.46 (dd, *J* = 1.8, 0.9 Hz, 1H), 7.31 (t, *J* = 7.6 Hz, 1H), 7.22 – 7.06 (m, 6H), 7.06 – 6.94 (m, 2H), 6.47 (dd, *J* = 3.5, 1.8 Hz, 1H), 3.90 – 3.56 (m, 5H), 3.54 – 3.39 (m, 1H), 3.13 (dd, *J* = 12.6, 3.2 Hz, 1H), 3.07 – 2.91 (m, 2H), 2.62 – 2.45 (m, 2H), 2.07 (s, 3H), 0.97 (s, 3H). ¹³C NMR (101 MHz, CDCl₃) δ 159.18, 154.40, 147.85, 143.82, 137.57, 136.77, 135.74, 131.59, 130.93, 129.71, 128.76, 128.62, 128.60, 126.83, 116.73, 111.43, 61.90, 48.85, 31.36, 17.91, 15.76. C₂₆H₂₈N₆O₂, EI-MS: *m/z* (M+H⁺): 457.6 (calculated), 457.6 (found).

1-(furan-2-carbonyl)-4-(2-phenyl-1-{{1-[(1S)-1-phenylethyl]-1H-1,2,3,4-tetrazol-5-yl}ethyl)piperazine. (**5at**). Yield: 70.9%. ¹H NMR (400 MHz, CDCl₃) δ 7.48 – 7.41 (m, 1H), 7.35 – 7.14 (m, 5H), 7.12 – 6.95 (m, 4H), 6.93 – 6.83 (m, 2H), 6.51 – 6.37 (m, 1H), 5.69 (q, *J* = 7.0 Hz, 0.5H), 4.89 (q, *J* = 7.0 Hz, 0.5H), 4.09 – 3.95 (m, 1H), 3.84 – 3.64 (m, 2H), 3.56 – 3.42 (m, 2H), 3.41 – 3.30 (m, 1H), 3.26 – 3.11 (m, 1H), 2.77 – 2.68 (m, 1H), 2.66 – 2.57 (m, 1H), 2.54 – 2.29 (m, 2H), 1.94 (d, *J* = 7.0 Hz, 1.5H), 1.65 (d, *J* = 7.0 Hz, 1.5H). ¹³C NMR (101 MHz, CDCl₃) δ 159.11, 158.96, 153.62, 152.95, 147.81, 143.85, 143.73, 139.92, 139.20, 137.36, 137.28, 129.32, 129.22, 129.14, 129.07, 128.86, 128.62, 128.52, 128.49, 127.06, 126.54, 126.12, 125.86, 116.78, 116.53, 111.44, 111.34, 61.69, 61.05, 58.44, 58.31, 35.78, 33.07, 22.56, 22.17. C₂₆H₂₈N₆O₂. EI-MS: *m/z* (M+H⁺): 457.6 (calculated), 457.6 (found).

1-[1-(1-benzyl-1H-1,2,3,4-tetrazol-5-yl)-2-phenylethyl]-4-(furan-2-carbonyl)piperazine. (**5au**). Yield: 87.3%. ¹H NMR (400 MHz, CDCl₃) δ 7.50 – 7.40 (m, 1H), 7.36 – 7.21 (m, 3H), 7.21 – 7.09 (m, 3H), 7.04 – 6.88 (m, 5H), 6.51 – 6.40 (m, 1H), 5.38 (d, *J* = 15.5 Hz, 1H), 5.00 (d, *J* = 15.5 Hz, 1H), 4.03 (dd, *J* = 10.6, 3.9 Hz, 1H), 3.76 – 3.48 (m, 4H), 3.37 (dd, *J* = 13.0, 10.6 Hz, 1H), 3.20 (dd, *J* = 13.0, 3.9 Hz, 1H), 2.69 – 2.42 (m, 4H). ¹³C NMR (101 MHz, CDCl₃) δ

159.06, 153.70, 147.85, 143.81, 137.30, 133.55, 129.26, 129.22, 128.86, 128.79, 127.31, 126.92, 116.71, 111.42, 61.40, 50.80, 49.20, 34.46. C₂₅H₂₆N₆O₂, EI-MS: m/z (M+H⁺): 443.5 (calculated), 443.6 (found).

1-(furan-2-carbonyl)-4-(1-{1-[(4-methylbenzenesulfonyl)methyl]-1H-1,2,3,4-tetrazol-5-yl}-2-phenylethyl)piperazine. (**5av**). Yield: 74.8%. ¹H NMR (400 MHz, CDCl₃) δ 7.46 (dd, *J* = 1.8, 0.9 Hz, 1H), 7.34 – 7.13 (m, 9H), 6.98 (dd, *J* = 3.5, 0.9 Hz, 1H), 6.46 (dd, *J* = 3.5, 1.8 Hz, 1H), 5.75 (d, *J* = 14.4 Hz, 1H), 5.36 (d, *J* = 14.4 Hz, 1H), 4.80 (dd, *J* = 9.6, 4.7 Hz, 1H), 3.93 – 3.60 (m, 4H), 3.52 – 3.38 (m, 1H), 3.38 – 3.23 (m, 1H), 2.90 – 2.64 (m, 4H), 2.39 (s, 3H). ¹³C NMR (101 MHz, CDCl₃) δ 159.02, 155.08, 147.72, 146.81, 143.83, 137.38, 131.73, 130.39, 129.61, 128.72, 128.67, 126.89, 116.72, 111.39, 65.48, 60.58, 49.05, 32.77, 21.82. C₂₆H₂₈N₆O₄S. EI-MS: m/z (M+H⁺): 521.6 (calculated), 521.6 (found).

1-(furan-2-carbonyl)-4-(2-phenyl-1-{1-[(1S)-1-phenylethyl]-1H-1,2,3,4-tetrazol-5-yl}ethyl)piperazine. (**5aw**). Yield: 70.8%. ¹H NMR (400 MHz, CDCl₃) δ 7.53 – 7.37 (m, 1H), 7.35 – 7.14 (m, 5H), 7.14 – 6.96 (m, 4H), 6.96 – 6.78 (m, 2H), 6.54 – 6.38 (m, 1H), 5.68 (q, *J* = 7.1 Hz, 0.5H), 4.88 (q, *J* = 7.0 Hz, 0.5H), 4.11 – 3.93 (m, 1H), 3.88 – 3.60 (m, 2H), 3.60 – 3.41 (m, 2H), 3.41 – 3.28 (m, 1H), 3.28 – 3.07 (m, 1H), 2.84 – 2.67 (m, 1H), 2.67 – 2.56 (m, 1H), 2.57 – 2.28 (m, 2H), 1.94 (d, *J* = 7.1 Hz, 1.5H), 1.64 (d, *J* = 7.0 Hz, 1.5H). ¹³C NMR (101 MHz, CDCl₃) δ 159.13, 158.98, 153.63, 152.96, 147.82, 143.86, 143.75, 139.93, 139.21, 137.37, 137.29, 129.33, 129.24, 129.16, 129.08, 128.88, 128.64, 128.54, 128.51, 127.08, 126.55, 126.13, 125.87, 116.81, 116.56, 114.36, 111.46, 111.36, 61.72, 61.07, 58.46, 58.34, 49.13, 35.82, 33.08, 22.58, 22.18. C₂₆H₂₈N₆O₂, EI-MS: m/z (M+H⁺): 457.6 (calculated), 457.6 (found).

1-[(5-methylthiophen-2-yl)({1-[(1S)-1-phenylethyl]-1H-1,2,3,4-tetrazol-5-yl})methyl]-4-(pyridin-2-yl)piperazine. (**5ax**). Yield: 87.9%. ¹H NMR (400 MHz, CDCl₃) δ 8.21 – 8.06 (m, 1H), 7.49 – 7.37 (m, 1H), 7.37 – 7.13 (m, 5H), 6.68 (dd, *J* = 3.6, 1.3 Hz, 1H), 6.65 – 6.46 (m, 3H), 6.18 (q, *J* = 7.1 Hz, 0.5H), 5.66 (q, *J* = 7.0 Hz, 0.5H), 5.13 (s, 0.5H), 5.10 (s, 0.5H), 3.52 – 3.26 (m, 4H), 2.67 – 2.58 (m, 1H), 2.56 – 2.48 (m, 1H), 2.49 – 2.30 (m, 5H), 2.05 – 1.91 (m, 3H). ¹³C NMR (101 MHz, CDCl₃) δ 159.24, 159.22, 153.70, 153.47, 147.95, 147.90, 141.79, 141.51, 139.60, 139.37, 137.53, 137.47, 133.53, 133.05, 129.15, 129.12, 128.91, 128.66, 128.61, 128.43, 126.44, 126.27, 124.81, 124.69, 113.54, 113.32, 107.12, 107.00, 60.65, 59.73, 59.06, 58.73, 50.23, 49.65, 45.08, 44.99, 22.84, 22.77, 15.40, 15.37. C₂₄H₂₇N₇S, EI-MS: m/z (M+H⁺): 446.6 (calculated), 446.8 (found).

1-[(5-methylthiophen-2-yl)({1-[(1S)-1-phenylethyl]-1H-1,2,3,4-tetrazol-5-yl})methyl]-4-[3-(trifluoromethyl)pyridin-2-yl]piperazine. (**5ay**). Yield: 74.6%. ¹H NMR (400 MHz, CDCl₃) δ 8.49 – 8.32 (m, 1H), 7.90 – 7.74 (m, 1H), 7.43 – 7.22 (m, 5H), 7.04 – 6.88 (m, 1H), 6.77 – 6.67 (m, 1H), 6.64 – 6.53 (m, 1H), 6.22 (q, *J* = 7.1 Hz, 0.5H), 5.74 (q, *J* = 7.0 Hz, 0.5H), 5.14 (s, 0.5H), 5.12 (s, 0.5H), 3.33 – 3.11 (m, 4H), 2.73 – 2.54 (m, 2H), 2.54 – 2.39 (m, 5H), 2.11 – 1.94 (m, 3H). ¹³C NMR (101 MHz, CDCl₃) δ 159.39, 159.22, 153.81, 153.53, 151.08, 150.98, 141.78, 141.50, 139.57, 139.45, 137.34, 137.29, 134.14, 133.20, 129.15, 128.87, 128.66, 128.64, 128.29, 126.51, 126.37, 124.82, 124.70, 117.08, 116.72, 116.60, 116.46, 60.68, 59.92, 59.09, 58.73, 50.48, 50.46, 50.31, 50.11, 22.89, 22.78, 15.43, 15.41. C₂₅H₂₆F₃N₇S, EI-MS: m/z (M+H⁺): 514.6 (calculated), 514.6 (found).

1-benzoyl-4-[(1-benzyl-1H-1,2,3,4-tetrazol-5-yl)(5-methylthiophen-2-yl)methyl]piperazine. (**5az**). Yield: 80.4%. ¹H NMR (400 MHz, CDCl₃) δ 7.47 – 7.28 (m, 8H), 7.20 – 7.03 (m, 2H), 6.69 – 6.49 (m, 2H), 5.73 (d, *J* = 15.4 Hz, 1H), 5.45 (d, *J* = 15.4 Hz, 1H), 5.07 (s, 1H), 3.87 – 3.03 (m, 4H), 2.68 – 2.48 (m, 2H), 2.45 (s, 3H), 2.43 – 2.17 (m, 2H). ¹³C NMR (101 MHz, CDCl₃) δ 170.29, 153.71, 142.06, 135.55, 133.40, 132.80, 129.86, 129.30, 129.08, 128.83, 128.54, 127.52, 127.15, 124.94, 59.65, 51.52, 49.96, 15.45. C₂₅H₂₆N₆O₂, EI-MS: *m/z* (M+H⁺): 459.6 (calculated), 459.4 (found).

1-benzoyl-4-[(5-methylthiophen-2-yl)(1-[(1S)-1-phenylethyl]-1H-1,2,3,4-tetrazol-5-yl)methyl]piperazine. (**5ba**). Yield: 81.7%. ¹H NMR (400 MHz, CDCl₃) δ 7.48 – 7.23 (m, 8H), 7.22 – 7.11 (m, 2H), 6.67 – 6.59 (m, 1H), 6.59 – 6.56 (m, 0.5H), 6.54 – 6.48 (m, 0.5H), 6.06 (q, *J* = 7.0 Hz, 0.5H), 5.53 (q, *J* = 7.0 Hz, 0.5H), 5.13 (s, 0.5H), 5.07 (s, 0.5H), 3.80 – 3.45 (m, 2H), 3.42 – 3.05 (m, 2H), 2.66 – 2.44 (m, 2H), 2.45 (s, 1.5H), 2.42 (s, 1.5H), 2.43 – 2.17 (m, 2H), 2.03 – 1.93 (m, 3H). ¹³C NMR (101 MHz, CDCl₃) δ 170.25, 170.16, 153.46, 153.24, 142.06, 141.77, 139.70, 139.13, 135.56, 135.43, 133.21, 132.97, 129.84, 129.73, 129.26, 129.13, 128.98, 128.76, 128.66, 128.50, 128.44, 127.08, 127.06, 126.31, 126.07, 124.89, 124.77, 60.24, 59.25, 59.06, 58.82, 50.37, 22.73, 22.70, 15.42, 15.36. C₂₆H₂₈N₆O₂, EI-MS: *m/z* (M+H⁺): 473.6 (calculated), 473.6 (found).

1-benzoyl-4-[[1-(2,6-dimethylphenyl)-1H-1,2,3,4-tetrazol-5-yl](5-methylthiophen-2-yl)methyl]piperazine. (**5bb**). Yield: 78.3%. ¹H NMR (400 MHz, CDCl₃) δ 7.45 – 7.30 (m, 6H), 7.26 – 7.22 (m, 1H), 7.18 – 7.08 (m, 1H), 6.74 – 6.60 (m, 1H), 6.60 – 6.50 (m, 1H), 4.70 (s, 1H), 3.88 – 3.58 (m, 2H), 3.58 – 3.26 (m, 2H), 2.83 – 2.65 (m, 2H), 2.55 – 2.31 (m, 2H), 2.42 (s, 3H), 2.04 (s, 3H), 1.53 (s, 3H). ¹³C NMR (101 MHz, CDCl₃) δ 170.32, 154.75, 142.33, 136.56, 135.78, 135.60, 133.02, 131.61, 131.25, 129.87, 129.15, 129.06, 129.01, 128.55, 127.19, 124.88, 58.99, 17.83, 17.09, 15.47. C₂₆H₂₈N₆O₂, EI-MS: *m/z* (M+H⁺): 473.6 (calculated), 473.4 (found).

1-[[1-(2,6-dimethylphenyl)-1H-1,2,3,4-tetrazol-5-yl](5-methylthiophen-2-yl)methyl]-4-(2-methylphenyl)piperazine. (**5bc**). Yield: 85.6%. ¹H NMR (400 MHz, CDCl₃) δ 7.38 (t, *J* = 7.6 Hz, 1H), 7.30 – 7.22 (m, 1H), 7.20 – 7.08 (m, 3H), 7.03 – 6.89 (m, 2H), 6.69 (d, *J* = 3.5 Hz, 1H), 6.61 – 6.49 (m, 1H), 4.71 (s, 1H), 3.05 – 2.73 (m, 6H), 2.68 – 2.52 (m, 2H), 2.44 (s, 3H), 2.22 (s, 3H), 2.09 (s, 3H), 1.55 (s, 3H). ¹³C NMR (101 MHz, CDCl₃) δ 155.15, 151.33, 142.03, 136.59, 135.97, 133.91, 132.70, 131.82, 131.14, 128.99, 128.97, 128.91, 126.67, 124.76, 123.35, 119.13, 59.37, 51.79, 50.85, 17.97, 17.94, 17.12, 15.51. C₂₆H₃₀N₆S, EI-MS: *m/z* (M+H⁺): 459.6 (calculated), 459.6 (found).

1-[[1-(2,6-dimethylphenyl)-1H-1,2,3,4-tetrazol-5-yl](5-methylthiophen-2-yl)methyl]-4-(pyridin-2-yl)piperazine. (**5bd**). Yield: 73.1%. ¹H NMR (400 MHz, CDCl₃) δ 8.13 (ddd, *J* = 4.9, 2.0, 1.0 Hz, 1H), 7.49 – 7.33 (m, 2H), 7.25 – 7.21 (m, 1H), 7.18 – 7.12 (m, 1H), 6.69 (d, *J* = 3.5 Hz, 1H), 6.62 – 6.53 (m, 3H), 4.71 (s, 1H), 3.51 (t, *J* = 5.1 Hz, 4H), 2.86 – 2.66 (m, 2H), 2.63 – 2.46 (m, 2H), 2.42 (s, 3H), 2.05 (s, 3H), 1.56 (s, 3H). ¹³C NMR (101 MHz, CDCl₃) δ 154.92, 147.64, 142.10, 137.80, 136.45, 135.96, 133.24, 131.71, 131.17, 129.03, 129.01, 128.96, 124.77, 113.41, 107.27, 59.19, 50.02, 45.35, 17.84, 17.12, 15.45. C₂₄H₂₇N₇S, EI-MS: *m/z* (M+H⁺): 446.6 (calculated), 446.6 (found).

4-bromo-N-[3-({1-[(1S)-1-phenylethyl]-1H-1,2,3,4-tetrazol-5-yl}[4-(pyridin-2-yl)piperazin-1-yl)methyl]phenyl]benzamide. (**5be**). Yield: 71.3%. ¹H NMR (400 MHz, CDCl₃) δ 8.23 (d, *J* = 6.0 Hz, 1H), 8.16 – 8.02 (m, 1H), 7.83 – 7.66 (m, 3H), 7.65 – 7.50 (m, 3H), 7.49 – 7.34 (m, 1H), 7.34 – 7.16 (m, 4H), 7.16 – 7.05 (m, 1.5H), 7.01 – 6.88 (m, 0.5H), 6.68 – 6.41 (m, 2H), 6.07 (q, *J* = 7.0 Hz, 0.5H), 5.70 (q, *J* = 6.9 Hz, 0.5H), 4.84 (s, 0.5H), 4.78 (s, 0.5H), 3.54 – 3.43 (m, 2H), 3.43 – 3.28 (m, 2H), 2.68 – 2.53 (m, 1H), 2.52 – 2.27 (m, 3H), 1.94 (d, *J* = 7.0 Hz, 1.5H), 1.88 (d, *J* = 7.0 Hz, 1.5H). ¹³C NMR (101 MHz, CDCl₃) δ 165.12, 165.01, 159.33, 159.30, 154.34, 153.86, 148.00, 147.97, 139.61, 139.18, 138.72, 138.43, 137.64, 137.60, 135.47, 134.72, 133.68, 133.61, 132.07, 132.04, 129.75, 129.40, 129.28, 129.18, 128.93, 128.91, 128.75, 128.72, 126.84, 126.75, 126.58, 126.21, 125.28, 120.94, 120.88, 120.61, 113.68, 113.60, 107.25, 107.16, 64.97, 64.94, 59.01, 58.82, 50.79, 50.72, 45.21, 45.11, 22.82, 22.72. C₃₂H₃₁BrN₈O, EI-MS: *m/z* (M+H⁺): 624.6 (calculated), 624.6 (found).

1-{{1-(2,6-dimethylphenyl)-1H-1,2,3,4-tetrazol-5-yl}(5-methylthiophen-2-yl)methyl}-4-[3-(trifluoromethyl)pyridin-2-yl]piperazine. (**5bf**). Yield: 69.3%. ¹H NMR (400 MHz, CDCl₃) δ 8.40 – 8.35 (m, 1H), 7.83 – 7.76 (m, 1H), 7.38 (t, *J* = 7.6 Hz, 1H), 7.27 – 7.22 (m, 1H), 7.18 – 7.11 (m, 1H), 6.97 – 6.89 (m, 1H), 6.74 – 6.66 (m, 1H), 6.60 – 6.53 (m, 1H), 4.73 (s, 1H), 3.47 – 3.08 (m, 4H), 2.91 – 2.71 (m, 2H), 2.70 – 2.51 (m, 2H), 2.43 (s, 3H), 2.07 (s, 3H), 1.55 (s, 3H). ¹³C NMR (101 MHz, CDCl₃) δ 159.31, 151.07, 137.37, 137.32, 136.50, 136.03, 131.73, 131.17, 129.03, 128.96, 125.41, 124.82, 116.81, 116.68, 116.37, 59.22, 50.49, 50.32, 17.89, 17.11, 15.49. C₂₅H₂₆F₃N₇S, EI-MS: *m/z* (M+H⁺): 514.6 (calculated), 514.6 (found).

1-(1-{{1-(2,6-dimethylphenyl)-1H-1,2,3,4-tetrazol-5-yl}(5-methylthiophen-2-yl)methyl}piperidin-4-yl)-2,3-dihydro-1H-1,3-benzodiazol-2-one. (**5bg**). Yield: 72.3%. ¹H NMR (400 MHz, CDCl₃) δ 10.29 (s, 1H), 7.40 (t, *J* = 7.6 Hz, 1H), 7.32 – 7.27 (m, 1H), 7.21 – 7.13 (m, 2H), 7.12 – 7.07 (m, 1H), 7.07 – 7.00 (m, 2H), 6.77 – 6.66 (m, 1H), 6.65 – 6.54 (m, 1H), 4.77 (s, 1H), 4.44 – 4.17 (m, 1H), 3.35 – 3.16 (m, 1H), 3.09 – 2.83 (m, 1H), 2.65 – 2.32 (m, 6H), 2.32 – 2.17 (m, 1H), 2.14 (s, 3H), 1.87 – 1.70 (m, 2H), 1.59 (s, 3H). ¹³C NMR (101 MHz, CDCl₃) δ 155.30, 155.08, 141.94, 136.44, 135.97, 133.57, 131.19, 129.02, 128.21, 124.78, 121.34, 121.11, 109.90, 109.63, 59.01, 51.48, 50.65, 48.84, 29.52, 29.25, 17.89, 17.16, 15.48. C₂₇H₂₉N₇O₂S, EI-MS: *m/z* (M+H⁺): 500.6 (calculated), 500.4 (found).

1-{{1-[(5-bromothiophen-2-yl)](1-[(1S)-1-phenylethyl]-1H-1,2,3,4-tetrazol-5-yl)methyl}piperidin-4-yl}-2,3-dihydro-1H-1,3-benzodiazol-2-one. (**5bh**). Yield: 70.1%. ¹H NMR (400 MHz, CDCl₃) δ 10.53 (s, 1H), 7.48 – 7.27 (m, 5H), 7.21 – 6.99 (m, 4H), 6.95 (d, *J* = 3.8 Hz, 0.5H), 6.87 (d, *J* = 3.8 Hz, 0.5H), 6.68 (d, *J* = 3.8 Hz, 0.5H), 6.56 (d, *J* = 3.8 Hz, 0.5H), 6.12 (q, *J* = 7.0 Hz, 0.5H), 5.76 (q, *J* = 7.0 Hz, 0.5H), 5.27 (s, 0.5H), 5.21 (s, 1H), 4.33 – 4.06 (m, 1H), 3.11 – 2.90 (m, 1H), 2.90 – 2.78 (m, 0.5H), 2.73 – 2.62 (m, 0.5H), 2.59 – 2.21 (m, 3H), 2.21 – 1.99 (m, 4H), 1.86 – 1.56 (m, 2H). ¹³C NMR (101 MHz, CDCl₃) δ 155.33, 155.31, 152.84, 152.74, 139.43, 139.21, 137.96, 137.56, 129.43, 129.34, 129.30, 129.28, 129.12, 129.00, 128.97, 128.84, 128.82, 128.72, 128.26, 128.19, 126.69, 126.27, 121.42, 121.31, 121.06, 120.95, 114.13, 113.82, 110.01, 109.90, 109.51, 109.12, 60.01, 59.26, 58.83, 51.00, 50.51, 50.19, 49.04, 48.55, 29.47, 29.20, 29.04, 22.82, 22.70. C₂₆H₂₆BrN₇O₂S, EI-MS: *m/z* (M+H⁺): 565.5 (calculated), 565.3 (found).

1-(1-{{5-(methylsulfonyl)thiophen-2-yl}}(1-[(1S)-1-phenylethyl]-1H-1,2,3,4-tetrazol-5-yl)methyl)piperidin-4-yl)-2,3-dihydro-1H-1,3-benzodiazol-2-one. (**5bi**). Yield: 68.2%. ¹H NMR (400 MHz, CDCl₃) δ 10.31 – 10.06 (2S, 1H), 7.55 – 7.22 (m, 5H), 7.22 – 6.98 (m, 4H), 6.98 – 6.63 (m, 2H), 6.17 (q, *J* = 7.0 Hz, 0.5H), 5.72 (q, *J* = 7.0 Hz, 0.5H), 5.21 (2S, 1H), 4.32 – 4.05 (m, 1H), 3.14 – 2.85 (m, 1H), 2.85 – 2.69 (m, 1H), 2.60 – 1.99 (m, 10H), 1.91 – 1.53 (m, 2H). ¹³C NMR (101 MHz, CDCl₃) δ 155.25, 153.29, 153.17, 139.63, 139.54, 139.33, 139.20, 138.03, 137.83, 129.91, 129.68, 129.50, 129.30, 129.27, 129.19, 129.09, 128.83, 128.80, 128.73, 128.22, 128.15, 126.74, 126.38, 126.32, 121.44, 121.33, 121.11, 121.04, 109.97, 109.86, 109.63, 109.24, 60.40, 59.53, 59.23, 58.81, 51.44, 50.59, 50.48, 49.25, 48.76, 29.54, 29.26, 29.16, 29.12, 22.85, 21.87, 21.72. C₂₇H₂₉N₇O₂, EI-MS: *m/z* (M+H⁺): 532.7 (calculated), 532.7 (found).

1-{{1-[(1-benzyl-1H-1,2,3,4-tetrazol-5-yl)(thiophen-2-yl)methyl]piperidin-4-yl}}-2,3-dihydro-1H-1,3-benzodiazol-2-one. (**5bj**). Yield: 86.3%. ¹H NMR (400 MHz, DMSO-*d*₆) δ 10.79 (s, 1H), 7.66 – 7.51 (m, 1H), 7.49 – 7.21 (m, 5H), 7.14 – 6.86 (m, 6H), 6.01 – 5.71 (m, 3H), 4.08 – 3.87 (m, 1H), 3.19 – 3.01 (m, 1H), 2.99 – 2.80 (m, 1H), 2.43 – 2.20 (m, 2H), 2.20 – 2.01 (m, 2H), 1.72 – 1.44 (m, 2H). ¹³C NMR (101 MHz, DMSO-*d*₆) δ 153.67, 153.61, 135.98, 134.81, 129.12, 128.75, 128.70, 128.22, 128.19, 127.80, 127.11, 126.30, 120.48, 120.24, 108.74, 108.51, 56.83, 50.27, 49.81, 47.61, 28.76, 28.50. C₂₅H₂₅N₇O₂, EI-MS: *m/z* (M+H⁺): 472.6 (calculated), 472.5 (found).

1-{{1-[(R)-{{1-[(1S)-1-phenylethyl]-1H-1,2,3,4-tetrazol-5-yl}}(thiophen-3-yl)methyl]piperidin-4-yl}}-2,3-dihydro-1H-1,3-benzodiazol-2-one. (**5bk**). Yield: 40.3%. The characterization of this compound was reported before.[23]

1-{{1-[(S)-{{1-[(1S)-1-phenylethyl]-1H-1,2,3,4-tetrazol-5-yl}}(thiophen-3-yl)methyl]piperidin-4-yl}}-2,3-dihydro-1H-1,3-benzodiazol-2-one. (**5bl**). Yield: 36.9%. The characterization of this compound was reported before.[23]

1-{{1-[(1-cyclohexyl-1H-1,2,3,4-tetrazol-5-yl)(thiophen-3-yl)methyl]piperidin-4-yl}}-2,3-dihydro-1H-1,3-benzodiazol-2-one. (**5bm**). Yield: 74.3%. The characterization of this compound was reported before.[23]

1-{{1-[(1-benzyl-1H-1,2,3,4-tetrazol-5-yl)(phenyl)methyl]piperidin-4-yl}}-2,3-dihydro-1H-1,3-benzodiazol-2-one. (**5bn**). Yield: 80.5%. ¹H NMR (400 MHz, DMSO-*d*₆) δ 10.80 (s, 1H), 7.52 – 7.42 (m, 2H), 7.42 – 7.26 (m, 6H), 7.26 – 7.17 (m, 2H), 7.13 – 7.03 (m, 1H), 7.03 – 6.87 (m, 3H), 5.84 (d, *J* = 3.3 Hz, 2H), 5.42 (s, 1H), 4.07 – 3.92 (m, 1H), 3.02 – 2.92 (m, 1H), 2.92 – 2.76 (m, 1H), 2.36 – 2.17 (m, 3H), 2.15 – 1.96 (m, 1H), 1.67 – 1.46 (m, 2H). ¹³C NMR (101 MHz, DMSO-*d*₆) δ 154.39, 153.64, 134.69, 134.64, 129.20, 129.13, 128.72, 128.26, 128.23, 128.17, 127.72, 120.48, 120.29, 108.74, 108.60, 79.16, 61.98, 50.20, 49.93, 49.88, 49.01, 28.72, 28.56. C₂₇H₂₇N₇O, EI-MS: *m/z* (M+H⁺): 466.6 (calculated), 466.6 (found).

1-{{1-[(1-benzyl-1H-1,2,3,4-tetrazol-5-yl)(2-methylphenyl)methyl]piperidin-4-yl}}-2,3-dihydro-1H-1,3-benzodiazol-2-one. (**5bo**). ¹H NMR (400 MHz, CDCl₃) δ 10.21 (s, 1H), 7.39 – 6.98 (m, 13H), 5.78 – 5.50 (m, 1H), 5.36 – 5.04 (m, 2H), 4.41 – 4.19 (m, 1H), 2.99 – 2.77 (m, 1H), 2.77 – 2.56 (m, 2H), 2.54 – 2.29 (m, 5H), 2.29 – 2.08 (m, 1H), 1.84 – 1.58 (m, 2H). ¹³C NMR (101 MHz, CDCl₃) δ 155.25, 154.11, 137.74, 133.33, 131.57, 129.16, 128.93, 128.68, 128.21, 127.43,

126.26, 121.36, 121.06, 109.92, 109.43, 60.92, 51.31, 51.16, 50.95, 49.06, 29.49, 19.48.
C₂₈H₂₉N₇O, EI-MS: m/z (M+H⁺): 480.6 (calculated), 480.6 (found).

1-{1-[phenyl({1-[(1S)-1-phenylethyl]-1H-1,2,3,4-tetrazol-5-yl})methyl]piperidin-4-yl}-2,3-dihydro-1H-1,3-benzodiazol-2-one. (**5bp**). Yield: 71.3%. ¹H NMR (400 MHz, CDCl₃) δ 10.27 (s, 0.5H), 10.22 (s, 0.5H), 7.48 – 6.92 (m, 1H), 6.03 (q, *J* = 7.0 Hz, 0.5H), 5.52 (q, *J* = 7.0 Hz, 0.5H), 4.99 (s, 0.5H), 4.83 (s, 0.5H), 4.36 – 4.08 (m, 1H), 3.24 – 3.06 (m, 0.5H), 2.97 – 2.75 (m, 1H), 2.71 – 2.62 (m, 0.5H), 2.60 – 2.21 (m, 3H), 2.21 – 2.01 (m, 1H), 1.99 – 1.83 (m, 3H), 1.83 – 1.60 (m, 2H). ¹³C NMR (101 MHz, CDCl₃) δ 155.32, 154.50, 154.06, 139.55, 139.17, 134.59, 134.34, 129.29, 129.21, 129.17, 129.09, 129.00, 128.97, 128.80, 128.74, 128.67, 128.22, 128.13, 126.60, 126.22, 121.44, 121.34, 121.11, 110.00, 109.87, 109.75, 109.40, 64.86, 64.74, 58.79, 58.60, 51.54, 50.85, 50.75, 50.66, 50.50, 50.16, 29.42, 29.24, 29.05, 22.67, 22.61. C₂₈H₂₉N₇O, EI-MS: m/z (M+H⁺): 480.6 (calculated), 480.4 (found).

1-{1-[(2-methylphenyl)({1-[(1S)-1-phenylethyl]-1H-1,2,3,4-tetrazol-5-yl})methyl]piperidin-4-yl}-2,3-dihydro-1H-1,3-benzodiazol-2-one. (**5bq**). Yield: 87.3%. ¹H NMR (400 MHz, DMSO-*d*₆) δ 10.81 (2S, 1H), 7.45 – 7.29 (m, 1H), 7.29 – 7.09 (m, 8H), 7.09 – 6.85 (m, 4H), 6.19 (q, *J* = 6.8 Hz, 0.5H), 5.91 (q, *J* = 6.8 Hz, 0.5H), 5.53 (s, 0.5H), 5.41 (s, 0.5H), 4.19 – 3.97 (m, 1H), 3.16 – 2.99 (m, 0.5H), 2.74 – 1.99 (m, 8.5H), 1.79 (dd, *J* = 6.9, 2.7 Hz, 3H), 1.72 – 1.43 (m, 2H). ¹³C NMR (101 MHz, DMSO-*d*₆) δ 153.64, 153.61, 153.53, 153.28, 139.59, 139.26, 137.43, 137.13, 133.64, 133.61, 131.07, 130.84, 129.14, 129.12, 128.80, 128.62, 128.50, 128.41, 128.28, 128.24, 128.21, 128.14, 127.96, 127.86, 126.34, 126.17, 125.78, 125.58, 120.50, 120.47, 120.30, 108.77, 108.64, 108.52, 59.24, 59.18, 57.23, 50.39, 50.09, 50.02, 48.23, 48.03, 28.88, 28.70, 22.43, 22.08, 19.14, 18.98. C₂₉H₃₁N₇O, EI-MS: m/z (M+H⁺): 494.6 (calculated), 494.6 (found).

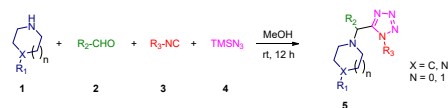
1-[1-({1-[(1S)-1-phenylethyl]-1H-1,2,3,4-tetrazol-5-yl})(1,2,3-thiadiazol-4-yl)methyl]piperidin-4-yl]-2,3-dihydro-1H-1,3-benzodiazol-2-one. (**5br**). Yield: 72.6%. ¹H NMR (400 MHz, CDCl₃) δ 10.28 (s, 0.7H), 10.25 (s, 0.3H), 9.28 (s, 0.7H), 9.13 (s, 0.3H), 7.56 – 7.28 (m, 5H), 7.13 – 6.95 (m, 3.4H), 6.87 – 6.77 (m, 0.6H), 6.45 (q, *J* = 7.0 Hz, 0.3H), 6.14 (s, 0.7H), 6.04 (q, *J* = 7.0 Hz, 0.7H), 5.86 (s, 0.3H), 4.18 – 3.95 (m, 1H), 3.25 – 3.06 (m, 1H), 2.87 – 2.63 (m, 1H), 2.54 – 1.65 (m, 9H). ¹³C NMR (101 MHz, CDCl₃) δ 155.23, 155.16, 152.43, 152.38, 139.55, 139.29, 137.99, 137.84, 129.41, 129.22, 129.16, 128.92, 128.76, 128.20, 128.12, 126.57, 126.38, 121.50, 121.39, 121.12, 120.92, 110.00, 109.90, 109.50, 108.97, 59.55, 58.92, 57.82, 56.98, 52.43, 52.06, 50.47, 50.31, 47.58, 46.80, 29.46, 29.39, 29.08, 28.67, 22.99, 22.78. C₂₄H₂₅N₉OS, EI-MS: m/z (M+H⁺): 488.6 (calculated), 488.5 (found).

1-{1-[(2,1,3-benzoxadiazol-5-yl)({1-[(1S)-1-phenylethyl]-1H-1,2,3,4-tetrazol-5-yl})methyl]piperidin-4-yl}-2,3-dihydro-1H-1,3-benzodiazol-2-one. (**5bs**). Yield: 69.8%. ¹H NMR (400 MHz, DMSO-*d*₆) δ 10.80 (2S, 1H), 8.22 – 8.03 (m, 1H), 8.02 – 7.82 (m, 1H), 7.70 – 7.57 (m, 0.5H), 7.52 – 7.46 (m, 0.5H), 7.47 – 7.28 (m, 2.5H), 7.27 – 7.05 (m, 3H), 7.02 – 6.91 (m, 3.5H), 6.32 (qd, *J* = 7.0, 1.8 Hz, 1H), 5.63 (2S, 1H), 4.22 – 4.04 (m, 0.5H), 4.03 – 3.83 (m, 0.5H), 3.17 – 3.03 (m, 0.5H), 2.98 – 2.79 (m, 1H), 2.79 – 2.66 (m, 0.5H), 2.50 – 2.31 (m, 2H), 2.31 – 2.16 (m, 1H), 2.16 – 1.80 (m, 4H), 1.73 – 1.32 (m, 2H). ¹³C NMR (101 MHz, DMSO-*d*₆) δ 153.67, 153.57, 152.71, 152.67, 148.70, 148.49, 148.35, 148.27, 140.02, 139.89, 139.81, 139.53, 134.04, 133.25, 129.23, 129.03, 128.80, 128.62, 128.27, 128.20, 128.12, 127.95, 126.43,

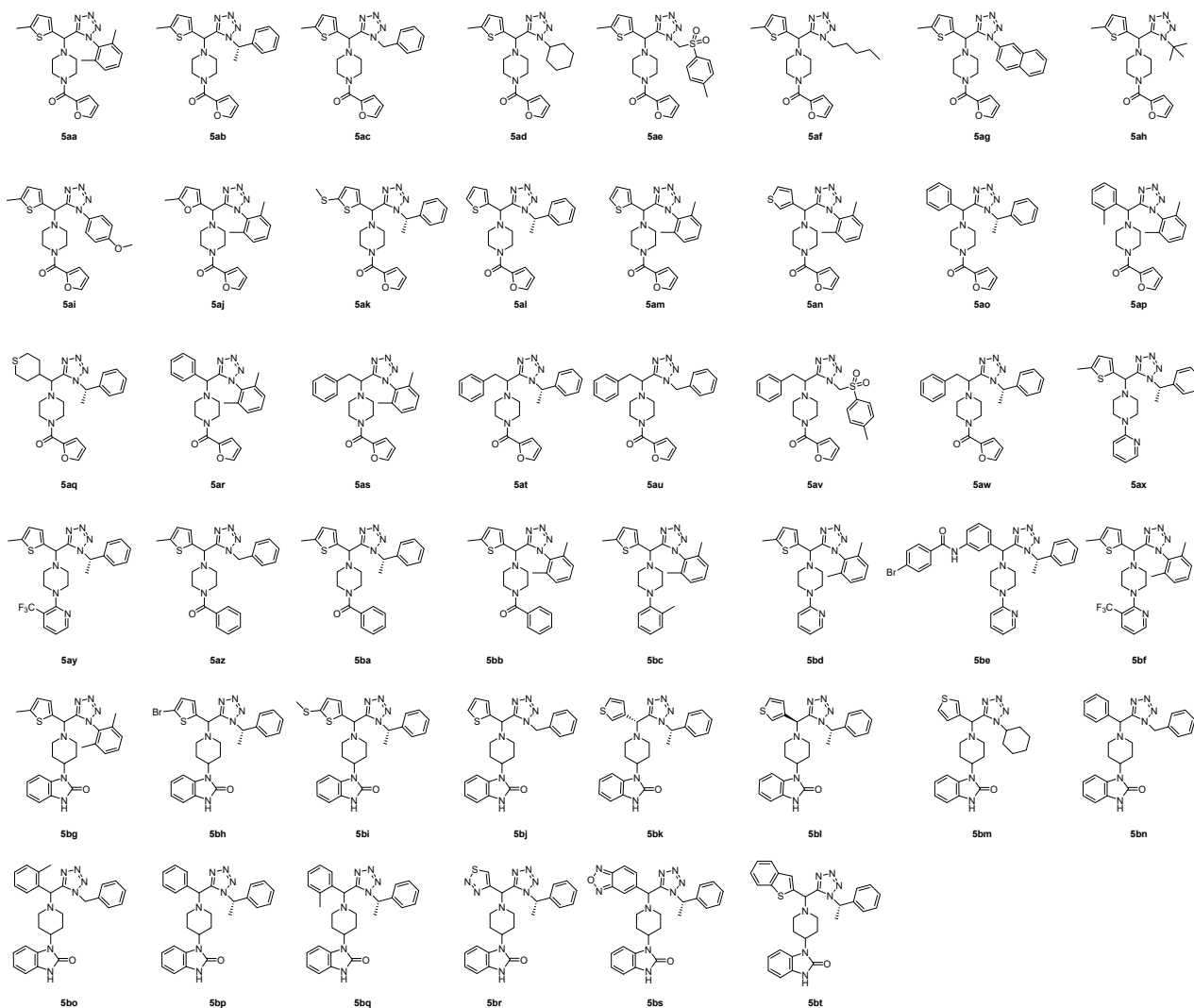
126.18, 120.50, 120.33, 120.23, 116.11, 115.79, 115.54, 108.75, 108.60, 108.52, 61.48, 61.24, 57.34, 57.20, 49.84, 49.74, 49.63, 49.26, 48.94, 28.74, 28.49, 22.40, 22.10. C₂₈H₂₇N₉O₂, EI-MS: m/z (M+H⁺): 522.6 (calculated), 522.6 (found).

1-{1-[(1-benzothiophen-2-yl)({1-[(1S)-1-phenylethyl]-1H-1,2,3,4-tetrazol-5-yl)methyl]piperidin-4-yl}-2,3-dihydro-1H-1,3-benzodiazol-2-one. (**5bt**). Yield: 72.3%. ¹H NMR (400 MHz, CDCl₃) δ 10.03 (2S, 1H), 7.54 – 7.22 (m, 7.5H), 7.22 – 7.00 (m, 5H), 7.00 – 6.85 (m, 1.5H), 6.22 (q, *J* = 7.0 Hz, 0.5H), 5.67 (q, *J* = 7.0 Hz, 0.5H), 5.31 (s, 0.5H), 5.27 (s, 0.5H), 4.33 – 4.10 (m, 1H), 3.14 – 3.00 (m, 0.5H), 3.00 – 2.88 (m, 0.5H), 2.88 – 2.71 (m, 1H), 2.64 – 2.31 (m, 2H), 2.31 – 2.12 (m, 1H), 2.12 – 1.98 (m, 3H), 1.90 – 1.54 (m, 3H). ¹³C NMR (101 MHz, CDCl₃) δ 155.18, 153.73, 153.54, 139.59, 139.37, 136.35, 136.13, 129.32, 129.25, 129.13, 128.84, 128.81, 128.77, 128.50, 128.19, 128.11, 127.02, 126.84, 126.75, 126.67, 126.45, 126.34, 121.44, 121.33, 121.12, 121.07, 109.94, 109.82, 109.70, 109.28, 60.19, 59.25, 59.19, 58.78, 51.59, 50.63, 50.55, 49.35, 48.77, 29.56, 29.26, 29.15, 22.87, 22.80. C₃₀H₂₉N₇O₅, EI-MS: m/z (M+H⁺): 536.7 (calculated), 536.5 (found).

A. General procedure for the synthesis tetrazole analogs by Ugi-Azide four-component reaction

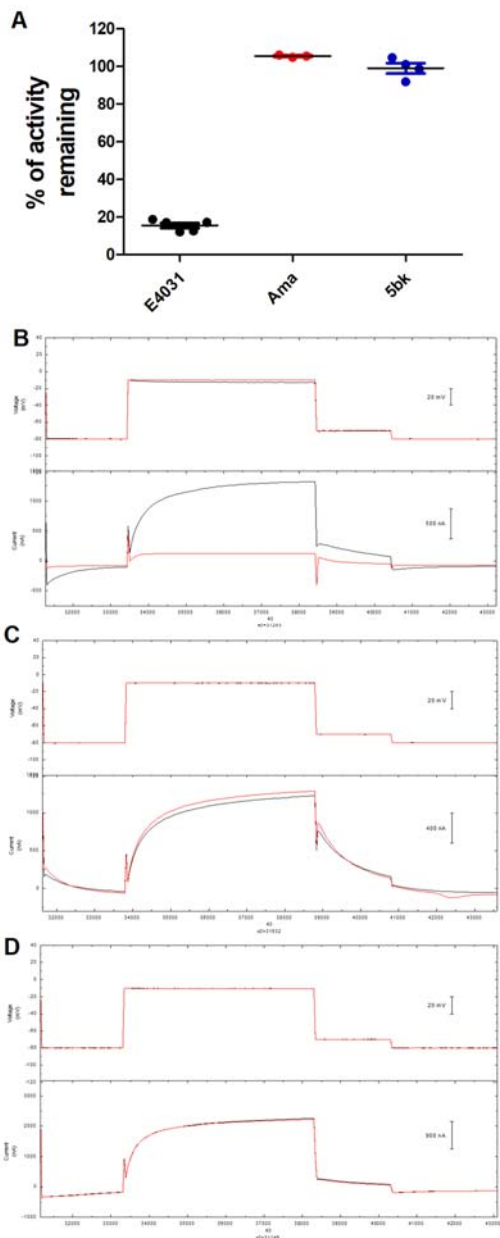


B. List of compounds synthesized and tested in the Ca²⁺ flux assay

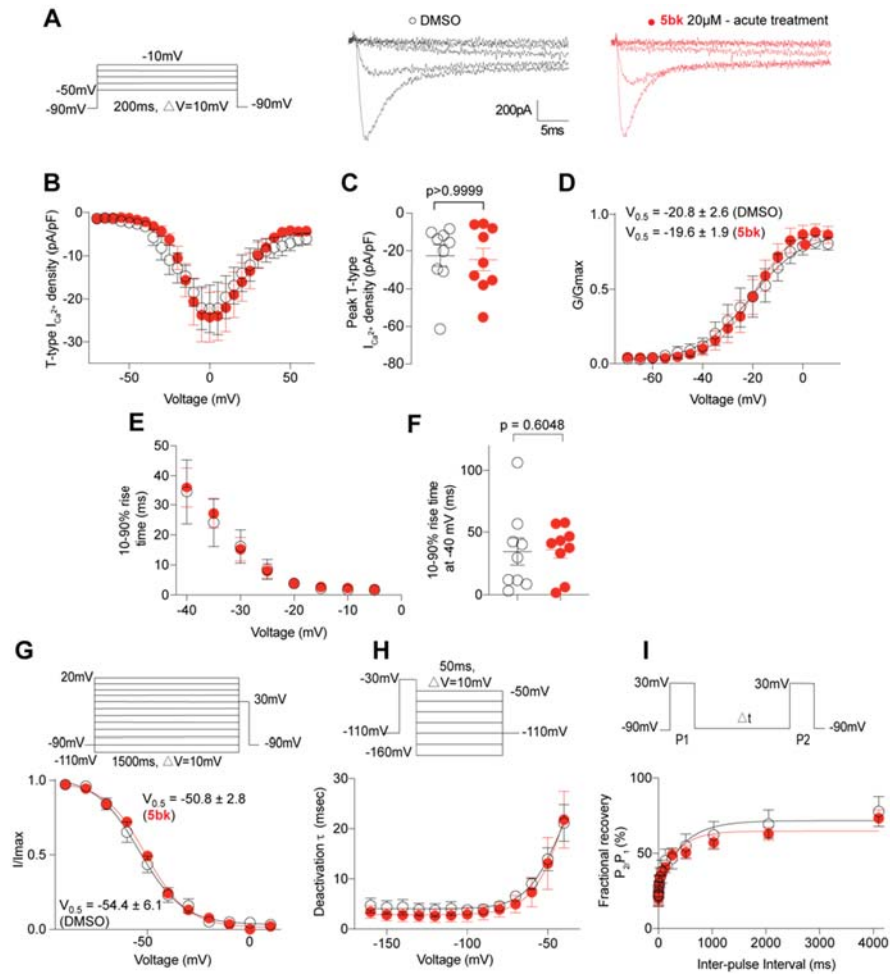


Supplementary Figure. 1. Synthesis of compounds by the Ugi-Azide four-component reaction.

(A) Synthesis methodology. (B) List of compounds synthesized and tested. **5bk** is also referred to as UAWJ111 throughout this **Supplementary Materials** section.

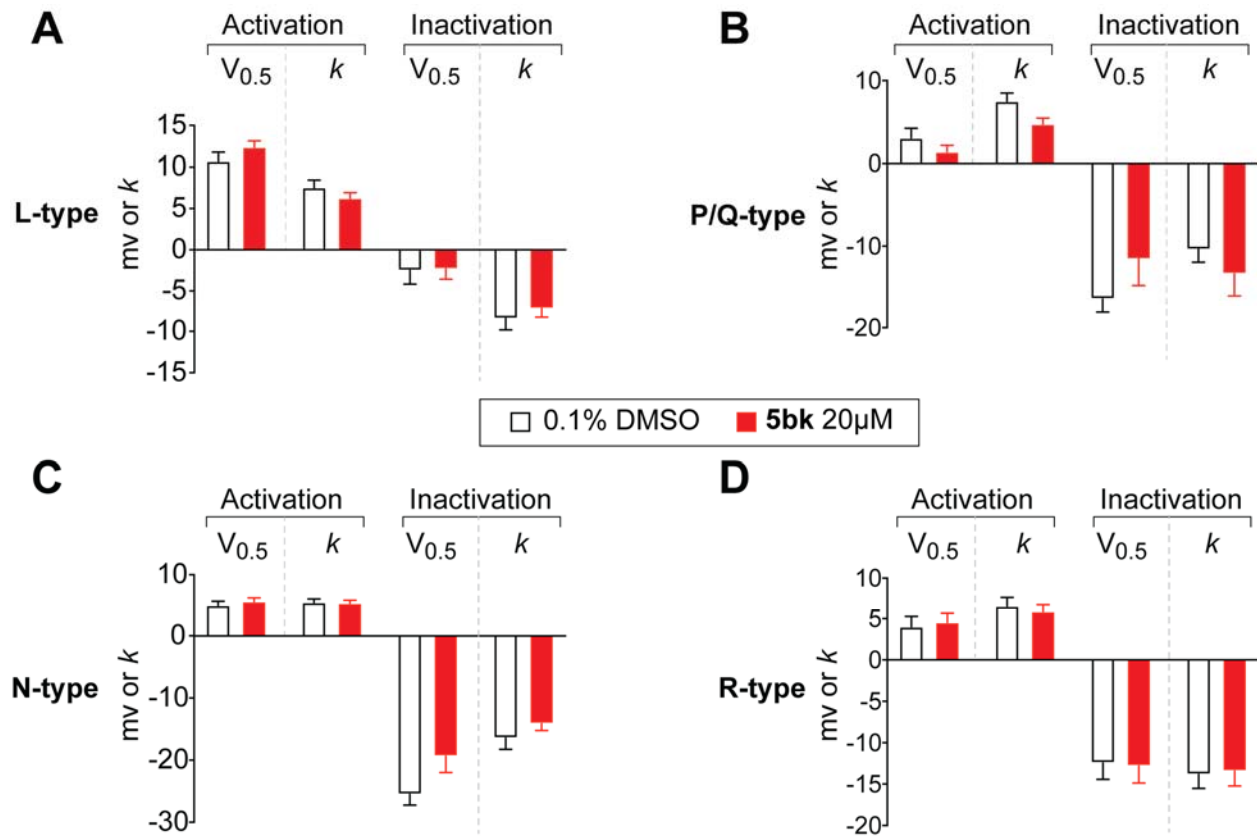


Supplementary Figure 3. 5bk does not affect hERG channels. hERG channel was expressed in oocytes and the current was recorded with and without 100 μ M of the indicated compounds. (A) Summary data of % hERG current remaining with the various compounds. E4031, a known hERG channel blocker, was used as a positive control [20]. Amantadine was used as a negative control. Representative traces from oocytes treated with vehicle (0.01% DMSO, *black trace*) or E4031 (B, *red trace*), Ama (C, *red trace*), or **5bk** (D, *red trace*).



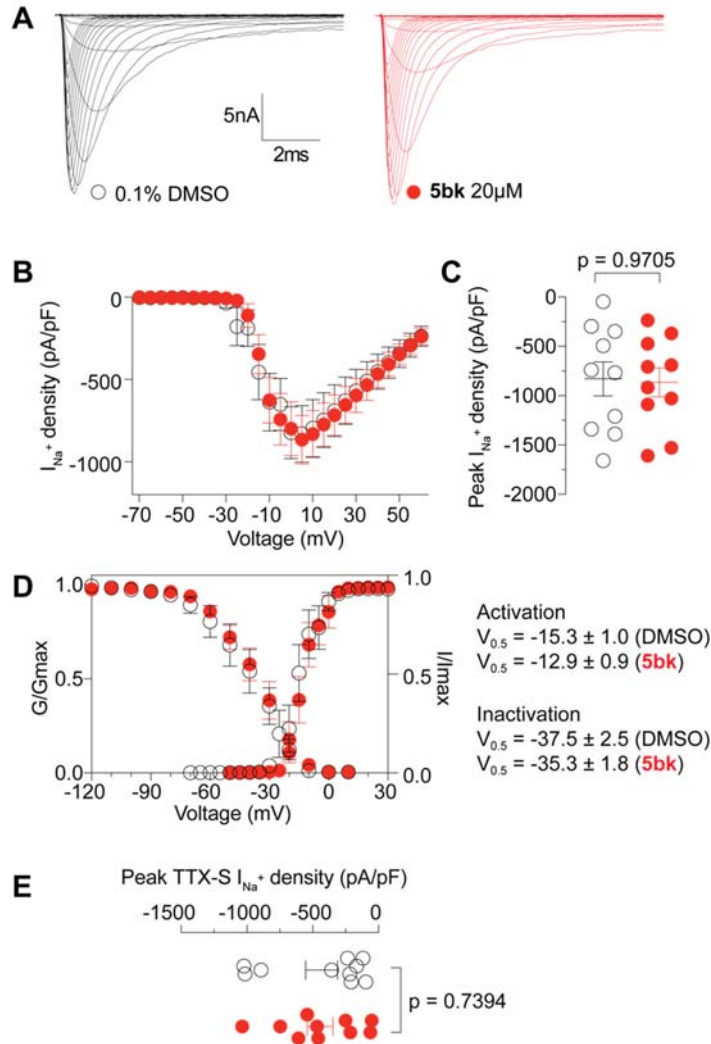
Supplementary Figure 4. Acute (<10 min) treatment with 5bk does not inhibit T-Type Ca^{2+} currents in dorsal root ganglion (DRG) sensory neuron. **(A)** Representative family of traces of T-Type Ca^{2+} currents from DRG sensory treated acutely (<10 min) with vehicle (0.01% DMSO) or 5bk (20 μM). Voltage protocol used to evoke the currents is shown. **(B)** Summary of the normalized (pA/pF) T-Type calcium current density versus voltage relationship and **(C)** peak T-Type Ca^{2+} current density at -10 mV (mean \pm SEM) from DRG sensory neurons treated as indicated. **(D)** Boltzmann fits for normalized conductance G/G_{max} voltage relations for voltage dependent activation of T-type currents. **(E)** Time-dependent activation (10-90% rise time) from I-V curves and at -40mV **(F)** in DRG cells shown calculated from the data in **B**. **(G)** Boltzmann fits for normalized conductance G/G_{max} voltage relations for voltage dependent inactivation of sensory neurons treated as indicated. **(H)** Deactivating tail currents in DRG neurons treated acutely with vehicle (0.01% DMSO) or 5bk (20 μM) were fit with a single-exponential function. The resulting τ values are plotted. **(I)** Recovery from inactivation in indicated groups. Data are

averaged and fitted by double exponential association (p values as indicated, Mann-Whitney test).
All graphs show mean \pm s.e.m. with individual data points showed when possible.

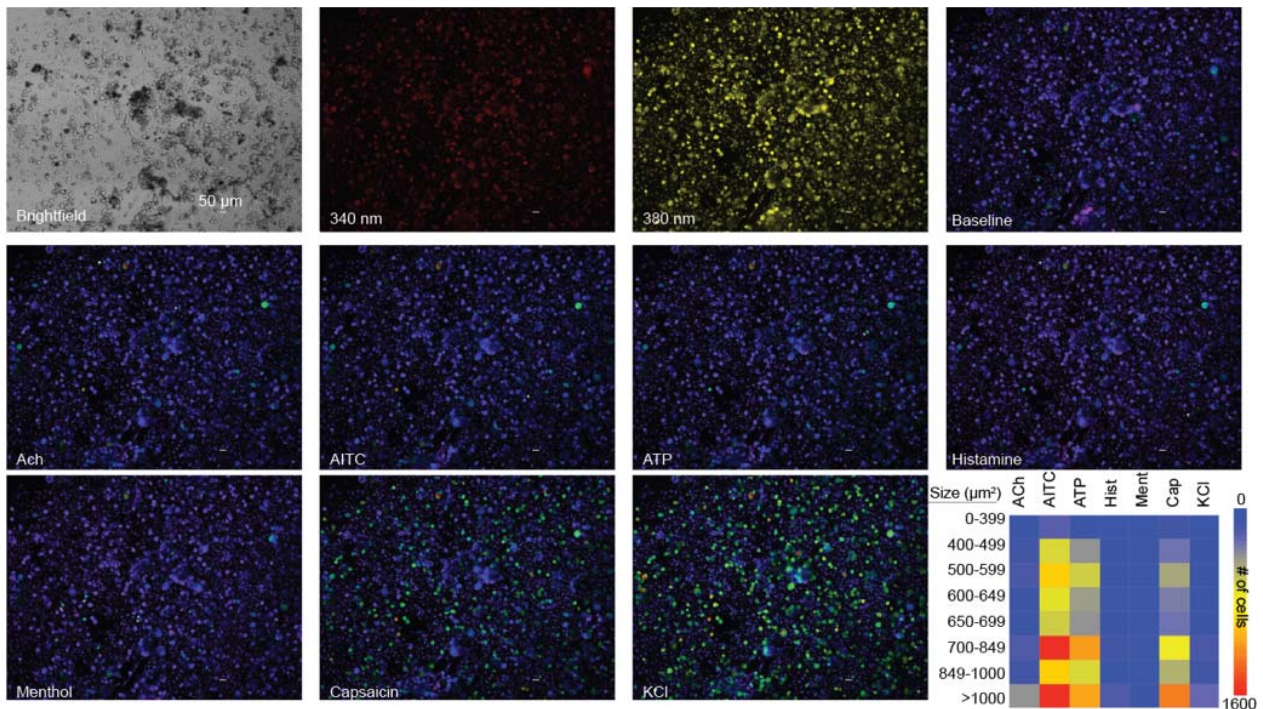


One-way ANOVA with Tukey's post hoc analysis: No comparisons significant

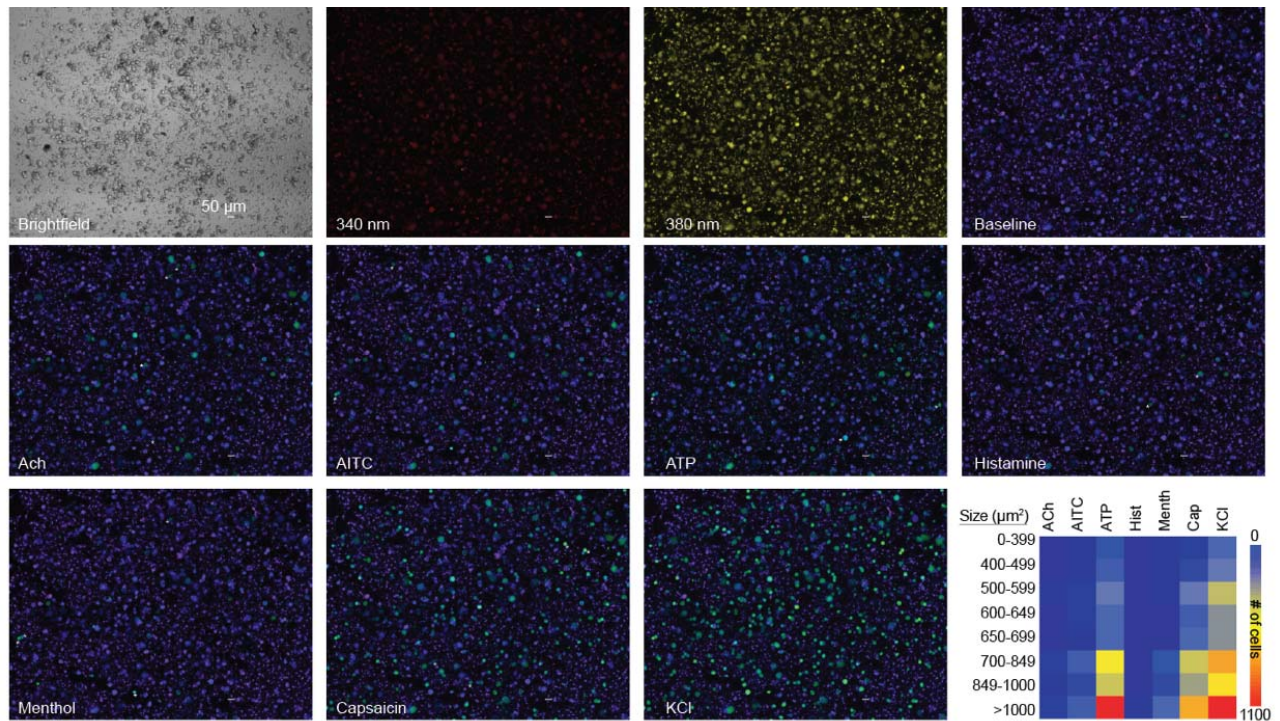
Supplementary Figure 5. Boltzmann fits for normalized conductance G/G_{max} voltage relations for voltage dependent activation and inactivation (data shown in **Figure 3**) of the sensory neurons treated overnight as indicated with 0.01% DMSO or **5bk**. Half-maximal activation and inactivation ($V_{1/2}$) and slope values (k) for activation and inactivation for the various HVA subtypes of calcium channels.



Supplementary Figure 6. 5bk does not affect Na^+ currents in dorsal root ganglion (DRG) neurons. (A) Representative traces of Na^+ currents from DRG sensory neurons treated overnight with 0.1% DMSO (control) or 20 μM **5bk**. Currents were evoked by 150ms pulse between -70 and $+60$ mV. Summary of the normalized (pA/pF) sodium (B) current density versus voltage relationship and (C) peak Na^+ current density at -10 mV (mean \pm SEM) from DRG neurons treated as indicated. (D) Boltzmann fits for normalized conductance G/G_{max} voltage relations for voltage dependent activation and inactivation of sensory neurons treated as indicated. $V_{1/2}$ values for activation and inactivation are indicated and were not significantly different between the treatment conditions ($P > 0.05$, Mann-Whitney test). (E) Summary of the peak TTX-sensitive (F) Na^+ current density (mean \pm SEM) from DRG neurons treated as indicated. (p value as indicated, Mann-Whitney test). TTX-sensitive and TTX-resistant fractions were calculated as described in the Methods section.



Supplementary Figure 7. Representative images of vehicle-treated DRG neurons post-challenge with constellation pharmacology triggers. Differential interference contrast (DIC) and pseudocolored fluorescent images of DRG neurons treated with vehicle, visualized for Fura2-AM before and after stimulations with each of the constellation triggers: menthol (400 nM), histamine (50 μM), ATP (10 μM), AITC (200 μM), acetylcholine (1 mM), capsaicin (100 nM) and KCl (90 mM)) during Ca²⁺ imaging. Scale bar is 50 μm. Size heat map reports number of DRG neurons of indicated size (measured by neuronal area) responding to constellation triggers.



Supplementary Figure 8. Representative images of 5bk-treated DRG neurons post-challenge with constellation pharmacology triggers. Differential interference contrast (DIC) and pseudocolored fluorescent images of DRG neurons treated with **5bk** (20 μM), visualized for Fura2-AM before and after stimulations with each of the constellation triggers: menthol (400 nM), histamine (50 μM), ATP (10 μM), AITC (200 μM), acetylcholine (1 mM), capsaicin (100 nM) and KCl (90 mM)) during Ca²⁺ imaging. Scale bar is 50 μm. Size heat map reports number of DRG neurons of indicated size (measured by neuronal area) responding to constellation triggers.

References

- [1] Brittain JM, Duarte DB, Wilson SM, Zhu W, Ballard C, Johnson PL, Liu N, Xiong W, Ripsch MS, Wang Y, Fehrenbacher JC, Fitz SD, Khanna M, Park CK, Schmutzler BS, Cheon BM, Due MR, Brustovetsky T, Ashpole NM, Hudmon A, Meroueh SO, Hingtgen CM, Brustovetsky N, Ji RR, Hurley JH, Jin X, Shekhar A, Xu XM, Oxford GS, Vasko MR, White FA, Khanna R. Suppression of inflammatory and neuropathic pain by uncoupling CRMP-2 from the presynaptic Ca(2)(+) channel complex. *Nature medicine* 2011;17(7):822-829.
- [2] Chaplan SR, Bach FW, Pogrel JW, Chung JM, Yaksh TL. Quantitative assessment of tactile allodynia in the rat paw. *Journal of neuroscience methods* 1994;53(1):55-63.
- [3] Choe W, Messinger RB, Leach E, Eckle VS, Obradovic A, Salajegheh R, Jevtovic-Todorovic V, Todorovic SM. TTA-P2 is a potent and selective blocker of T-type calcium channels in rat sensory neurons and a novel antinociceptive agent. *MolPharmacol* 2011;80(5):900-910.
- [4] Dustrude ET, Moutal A, Yang X, Wang Y, Khanna M, Khanna R. Hierarchical CRMP2 posttranslational modifications control NaV1.7 function. *Proceedings of the National Academy of Sciences of the United States of America* 2016;113(52):E8443-E8452.
- [5] Dustrude ET, Wilson SM, Ju W, Xiao Y, Khanna R. CRMP2 protein SUMOylation modulates NaV1.7 channel trafficking. *The Journal of biological chemistry* 2013;288(34):24316-24331.
- [6] Francois-Moutal L, Wang Y, Moutal A, Cottier KE, Melemedjian OK, Yang X, Wang Y, Ju W, Largent-Milnes TM, Khanna M, Vanderah TW, Khanna R. A membrane-delimited N-myristoylated CRMP2 peptide aptamer inhibits CaV2.2 trafficking and reverses inflammatory and postoperative pain behaviors. *Pain* 2015;156(7):1247-1264.
- [7] Gray WR, Olivera BM, Cruz LJ. Peptide toxins from venomous *Conus* snails. *Annual review of biochemistry* 1988;57:665-700.
- [8] Huynh TN, Krigbaum AM, Hanna JJ, Conrad CD. Sex differences and phase of light cycle modify chronic stress effects on anxiety and depressive-like behavior. *Behavioural brain research* 2011;222(1):212-222.
- [9] Ibrahim MM, Patwardhan A, Gilbraith KB, Moutal A, Yang X, Chew LA, Largent-Milnes T, Malan TP, Vanderah TW, Porreca F, Khanna R. Long-lasting antinociceptive effects of green light in acute and chronic pain in rats. *Pain* 2017;158(2):347-360.
- [10] Khanna R, Yu J, Yang X, Moutal A, Chefdeville A, Gokhale V, Shuja Z, Chew LA, Bellampalli SS, Luo S, Francois-Moutal L, Serafini MJ, Ha T, Perez-Miller S, Park KD, Patwardhan A, Streicher JM, Colecraft HM, Khanna M. Targeting the CaV α - β interaction yields an antagonist of the N-type CaV2.2 channel with broad antinociceptive efficacy. *Pain* 2019.

- [11] Milligan ED, O'Connor KA, Nguyen KT, Armstrong CB, Twining C, Gaykema RP, Holguin A, Martin D, Maier SF, Watkins LR. Intrathecal HIV-1 envelope glycoprotein gp120 induces enhanced pain states mediated by spinal cord proinflammatory cytokines. *The Journal of neuroscience : the official journal of the Society for Neuroscience* 2001;21(8):2808-2819.
- [12] Mintz IM, Venema VJ, Swiderek KM, Lee TD, Bean BP, Adams ME. P-type calcium channels blocked by the spider toxin omega-Aga-IVA. *Nature* 1992;355(6363):827-829.
- [13] Moutal A, Chew LA, Yang X, Wang Y, Yeon SK, Telemi E, Meroueh S, Park KD, Shrinivasan R, Gilbraith KB, Qu C, Xie JY, Patwardhan A, Vanderah TW, Khanna M, Porreca F, Khanna R. (S)-lacosamide inhibition of CRMP2 phosphorylation reduces postoperative and neuropathic pain behaviors through distinct classes of sensory neurons identified by constellation pharmacology. *Pain* 2016;157(7):1448-1463.
- [14] Moutal A, Li W, Wang Y, Ju W, Luo S, Cai S, Francois-Moutal L, Perez-Miller S, Hu J, Dustrude ET, Vanderah TW, Gokhale V, Khanna M, Khanna R. Homology-guided mutational analysis reveals the functional requirements for antinociceptive specificity of collapsin response mediator protein 2-derived peptides. *British journal of pharmacology* 2017.
- [15] Moutal A, Wang Y, Yang X, Ji Y, Luo S, Dorame A, Bellampalli SS, Chew LA, Cai S, Dustrude ET, Keener JE, Marty MT, Vanderah TW, Khanna R. Dissecting the role of the CRMP2-neurofibromin complex on pain behaviors. *Pain* 2017;158(11):2203-2221.
- [16] Newcomb R, Szoke B, Palma A, Wang G, Chen X, Hopkins W, Cong R, Miller J, Urge L, Tarczy-Hornoch K, Loo JA, Dooley DJ, Nadasdi L, Tsien RW, Lemos J, Miljanich G. Selective peptide antagonist of the class E calcium channel from the venom of the tarantula *Hysterocrates gigas*. *Biochemistry* 1998;37(44):15353-15362.
- [17] Olson KM, Duron DI, Womer D, Fell R, Streicher JM. Comprehensive molecular pharmacology screening reveals potential new receptor interactions for clinically relevant opioids. *PloS one* 2019;14(6):e0217371.
- [18] Polomano RC, Mannes AJ, Clark US, Bennett GJ. A painful peripheral neuropathy in the rat produced by the chemotherapeutic drug, paclitaxel. *Pain* 2001;94(3):293-304.
- [19] Teichert RW, Schmidt EW, Olivera BM. Constellation pharmacology: a new paradigm for drug discovery. *Annual review of pharmacology and toxicology* 2015;55:573-589.
- [20] Vandenberg JI, Perry MD, Perrin MJ, Mann SA, Ke Y, Hill AP. hERG K(+) channels: structure, function, and clinical significance. *Physiol Rev* 2012;92(3):1393-1478.
- [21] Yaksh TL, Rudy TA. Chronic catheterization of the spinal subarachnoid space. *Physiology & behavior* 1976;17(6):1031-1036.

- [22] Yu J, Moutal A, Dorame A, Bellampalli SS, Chefdeville A, Kanazawa I, Pham NYN, Park KD, Weimer JM, Khanna R. Phosphorylated CRMP2 Regulates Spinal Nociceptive Neurotransmission. *Molecular neurobiology* 2018.
- [23] Zhang J, Hu Y, Foley C, Wang Y, Musharrafieh R, Xu S, Zhang Y, Ma C, Hulme C, Wang J. Exploring Ugi-Azide Four-Component Reaction Products for Broad-Spectrum Influenza Antivirals with a High Genetic Barrier to Drug Resistance. *Sci Rep* 2018;8(1):4653.